The severity of *SLC1A2*-associated neurodevelopmental disorders correlates with transporter dysfunction

Peter Kovermann,[a,p] Allan Bayat,[b,c,d,p] Christina D. Fenger,[d,e] Lisette Leeuwen,[f] Artem Borovikov,[g] Artem Sharkov,[h,i] Virginie Levrat,[j] Gaetan Lesca,[k,l] Laurence Perrin,[m] Jonathan Levy,[m,n] Christoph Fahlke,[a] Rikke S. Møller,[b,d] and Anders A. Jensen[o,*]

[a]Forschungszentrum Jülich GmbH, Institute of Biological Information Processing 1 (IBI-1), Molekular- und Zellphysiologie, Jülich D-52428, Germany
[b]Department of Regional Health Research, University of Southern Denmark, Odense M DK-5230, Denmark
[c]Department of Pediatrics, Danish Epilepsy Centre Filadelfia (member of ERN EpiCARE), Dianalund DK-4293, Denmark
[d]Department of Epilepsy Genetics and Personalized Medicine, Danish Epilepsy Centre Filadelfia (member of ERN EpiCARE), Dianalund DK-4293, Denmark
[e]Amplexa Genetics, Odense C DK-5000, Denmark
[f]Department of Genetics, University Medical Center Groningen, Groningen, the Netherlands
[g]Research Centre for Medical Genetics, Moscow, Russia
[h]Veltischev Research and Clinical Institute for Pediatrics and Pediatric Surgery of the Pirogov Russian National Research Medical University, Moscow, Russia
[i]Genomed Ltd., Moscow, Russia
[j]Service de Pédiatrie, Centre Hospitalier Annecy Genevois, Pringy, France
[k]Department of Medical Genetics, University Hospital of Lyon and Claude Bernard Lyon University, Lyon, France
[l]Pathophysiology and Genetics of Neuron and Muscle (PNMG), UCBL, CNRS UMR5261 - INSERM U1315, Lyon, France
[m]Department of Genetics, APHP Nord, Robert Debré University Hospital, Paris 75019, France
[n]Multi-site Medical Biology Laboratory SeqOIA-FMG2025, Paris 75014, France
[o]Department of Drug Design and Pharmacology, Faculty of Health and Medical Sciences, University of Copenhagen, Copenhagen Ø DK-2100, Denmark

eBioMedicine
2025;114: 105648
Published Online xxx
https://doi.org/10.1016/j.ebiom.2025.105648

Summary

Background Excitatory amino acid transporter 2 (EAAT2) is the predominant glutamate transporter and a key mediator of excitatory neurotransmission in the human brain. Here we present a cohort of 18 individuals harbouring 13 different *SLC1A2* variants, who all present with neurodevelopmental impairment with variable symptoms and disease severities, and we delineate the impact of these variants on EAAT2 function.

Methods The consequences of nine novel missense *SLC1A2* variants for expression, transport and anion channel properties of EAAT2 expressed in mammalian cells were characterized by confocal microscopy, enzyme-linked immunosorbent and [^{3}H]-D-aspartate uptake assays, and electrophysiological recordings.

Findings Ten of the 13 *SLC1A2* variants mediated significant changes to EAAT2 expression and/or function. These molecular phenotypes were classified into three categories: overall loss-of-function (F249Sfs*17, A432D, A439V, c.1421+1G>C), mild gain-of-anion-channel function (I276S, G360A), and mixed loss-of-transport/gain-of-anion-channel function (G82R, L85R, L85P, P289R). In contrast, L37P, H542R and I546T did not mediate significant changes to EAAT2 expression or function. Although specific clinical outcomes in individuals carrying variants within each category varied somewhat, the three categories overall translated into distinct clinical phenotypes in terms of phenotypic traits and severity.

Interpretation The observed associations between functional effects and clinical phenotypes produced by these variants offer valuable insights for future predictions of progression and severity of *SLC1A2*-associated neurodevelopmental disorders. Furthermore, these associations between variant-induced changes in EAAT2 function and phenotypic traits could assist in tailoring personalized treatments of these disorders.

Funding This work was funded by the German Ministry of Education and Research and by the Lundbeck Foundation.

*Corresponding author. Department of Drug Design and Pharmacology, Faculty of Health and Medical Sciences, University of Copenhagen, Universitetsparken 2, Copenhagen Ø DK-2100, Denmark.
E-mail address: aaj@sund.ku.dk (A.A. Jensen).
[p]Joined co-first authors.

Keywords: Epilepsy; *SLC1A2*; Excitatory amino acid transporter 2 (EAAT2); Genetic variants; Transporter uptake; Patch clamp; Phenotyping

Research in context

Evidence before this study

The excitatory amino acid transporter 2 (EAAT2) encoded by the *SLC1A2* gene is the predominant transporter for glutamate, the major excitatory neurotransmitter in the human brain. In addition to being responsible for the vast majority of total glutamate uptake in the central nervous system, EAAT2 also acts as a glutamate-gated anion channel, and thus it constitutes a key mediator of central excitatory neurotransmission. Genetic mutations (termed "variants") in *SLC1A2* have been associated with neurodevelopmental disorders, but only a few of these variants have been identified. Thus, genotype-phenotype correlations have not been reported for this gene, and it remains insufficiently understood how EAAT2 dysfunction results in the observed clinical phenotypes.

Added value of this study

In the present study, we have performed molecular and clinical analyses on 13 *SLC1A2* variants identified from 18 individuals presenting with a range of neurodevelopmental disorders. 10 of the 13 variants were found to cause substantial changes to the expression and/or function of EAAT2, and the molecular phenotypes displayed by these 10 variants could be classified into three distinct categories. Interestingly, the variants from the three categories translated into distinct clinical phenotypes in individuals harbouring them. Thus, the distinct clinical phenotypic traits and severity arising from these *SLC1A2* variants overall correlated with the changes in EAAT2 expression and function induced by them.

Implications of all the available evidence

Elucidation of the changes produced by genetic variants in the expression and functional properties of the encoded protein provides the foundation for understanding the clinical outcomes of variant-associated disorders. We propose that this detailed molecular and clinical analysis of all *SLC1A2* variants reported to date lay a solid foundation for future predictions of the progression and severity of neurodevelopmental disorders associated with this gene. We also hope that the observed associations between EAAT2 dysfunctions and the associated phenotypic traits identified here will assist in tailoring personalized treatments of these disorders.

Introduction

L-Glutamate (L-Glu) is the major excitatory neurotransmitter in the human brain, where it is involved in or contributes to essentially all central functions. Glutamatergic hyper- or hypofunction have been linked to a range of neurological, cognitive, and psychiatric disorders, and thus glutamatergic receptors, transporters and enzymes constitute promising therapeutic targets.[1–3]

Following its release from presynaptic terminals, L-Glu is quickly taken up into glia and neurons by five excitatory amino acid transporters (EAAT1-5) from solute carrier 1 (*SLC1*) family of Na^+-dependent transporters.[4–6] The EAAT functions as a homotrimeric assembly, with each monomer comprising intracellular amino- and carboxy-termini, eight transmembrane domains (TM1-8) and two hairpin structures (HP1-2) with interconnecting extra- and intracellular loops.[5,7,8] The transport domain (TM3,6–8, HP1-2) in the monomer mediates stoichiometrically coupled L-Glu transport via an elevator mechanism driven by co-transport of three Na^+ and one H^+ and counter-transport of one K^+, while the trimerization domain (TM1-2,4–5) is anchored to the plasma membrane making inter-monomeric contacts.[5,7–10] EAATs also act as anion channels that open and close during transitions along the L-Glu transport cycle via brief gap openings between the transport and trimerization domains.[11–15]

Variants in *SLC1A1-3* and *SLC1A6-7* encoding for the five EAATs have been linked with various neurological and neuropsychiatric disorders.[16,17] For example, we and others have found missense *SLC1A3* variants associated with episodic ataxia 6 to change EAAT1 anion channel conduction.[13,18–21] EAAT2, the predominant glial and presynaptic EAAT subtype, is abundantly expressed throughout the brain, where it mediates ~90% of total central L-Glu uptake,[4,22,23] which makes *SLC1A2* variants of potential importance for a range of central nervous system (CNS) disorders.[24–26] Recently, three missense *SLC1A2* variants associated with developmental and epileptic encephalopathies (DEEs)[27–30] were reported to significantly alter EAAT2 anion channel function.[24] However, the *SLC1A2*-related phenotype remains ill-defined, and genotype-phenotype correlations have not been reported.

With the present study we aim to provide the first genotype-phenotype correlation analysis for *SLC1A2*, to elucidate the molecular phenotypic basis for *SLC1A2*-associated neurodevelopmental disorders, and to provide the basis for future predictions of disease progression and severity of these. We present a cohort of

18 individuals with 13 presumed pathogenic *SLC1A2* variants presenting with neurodevelopmental disorders and DEEs. We delineate the effects induced by nine novel missense variants on EAAT2 expression and function via heterologous expression of wild-type (WT) and mutant transporters in mammalian cell lines, and we deep-phenotype the neurodevelopmental disorders and epileptology associated with *SLC1A2* variants.

Methods

Clinical and genetic ascertainment

Our cohort consists of 18 individuals with 13 presumed pathogenic *SLC1A2* variants; 11 novel and seven previously published[27–31] individuals, one for whom we provide additional clinical information. The novel individuals were recruited through a network of epilepsy and genetic centres in Europe and evaluated as previously described.[32] Gender information and clinical data were gathered by attending physicians using a structured questionnaire. Seizures, epilepsies, and epilepsy syndromes were classified according to the ILAE classification.[33,34] Data are reported in line with the Strengthening Reporting of Observational Studies in Epidemiology (STROBE) statement.

The *SLC1A2* variants were annotated using the transcript NM_004171.4 and classified according to the 2015 American College of Medical Genetics and Genomics (ACMG) guidelines.[35] The functional effects of the missense variants were predicted using Rare Exome Variant Ensemble Learner (REVEL)[36] and Combined Annotation Dependent Depletion (CADD).[37] The Genome Aggregation Database (gnomAD) v4.0[38,39] was used to obtain the frequencies of the variants that were described according to Human Genome Variation Society (HGVS) nomenclature recommendations[40] using Mutalyzer software (https://mutalyzer.nl/).

Molecular biology

The construction of pRcCMV-YFP-EAAT2 cDNA has been reported previously.[41] HA-EAAT2-pCDNA3.1 cDNA comprising the human EAAT2 with the haemagglutinin(HA)-epitope (YPYDVPDYA) inserted between E221 and V222 in the extracellular TM4b/4c loop (pcDNA3.1-HA-EAAT2) was generated by the overlap extension PCR technique,[42] and the epitope insertion in HA-EAAT2 was found to be functionally silent (data not shown). All point mutations in EAAT2 cDNAs (using the same codons for the variations as those in the genomic DNAs of the individuals in our cohort) were generated by PCR and verified by cDNA sequencing.

Cell culture and transfections

HEK293T and COS-7 cells (RRID: CVCL_0063 and CVCL_0224, respectively) were cultured in humidified atmosphere at 5% CO_2 and 37 °C. Transient transfections of HEK293T cells using the $Ca_3(PO_4)_2$ technique was performed as previously described.[41]

COS-7 cells were cultured in Dulbecco's Modified Eagle Medium Glutamax-I supplemented with penicillin (100 U/mL), streptomycin (100 µg/mL) and 5% dialysed foetal bovine serum (all obtained from Invitrogen, Paisley, UK). The COS-7 cells were split into poly-D-lysine-coated 48- or 96-well plates [using 1×10^5 cells and a total of 200 ng cDNA per 48w-well (ELISA) and 5×10^4 cells and a total of 100 ng cDNA per 96w-well ([^{3}H]-D-Asp uptake)] and transfected using Lipofectamine 2000 (Thermo Fisher Scientific, Waltham, MA) according to the protocol of the manufacturer. The specific cDNA quantities used in the transfections are given in the ELISA and [^{3}H]-D-Asp uptake assay methods described below, and mock-transfected cells (transfected in parallel with "empty" pCDNA3.1; 200 ng/48w-well and 100 ng/96w-well) were included in all experiments. 16–20 h after the transfections, the transfection medium was removed from the wells and substituted with fresh culture medium. The following day, 40–48 h after the transfection, the transfected cells were used for the experiments.

Confocal microscopy

HEK293T cells expressing mYFP- or mCherry-EAAT2 fusion proteins were singularized with Trypsin-EDTA (0.05%, Gibco, UK) and plated on poly-L-lysine-coated (0.1% in *dd*H_2O, 1 h, Sigma–Aldrich) coverslips 24 h after $Ca_3(PO_4)_2$ transfection.[20] Images were acquired with a Leica TCS SP5 inverted microscope (Wetzlar, Germany) in phosphate-buffered saline at room temperature (RT) 48 h after transfection. Images were analysed with Fiji image analysis software.[43]

Enzyme-linked immunosorbent assay (ELISA)

Total and cell surface expression levels of HA-tagged WT or variant EAAT2 in COS-7 cells were quantified by an ELISA performed as previously described.[44] Cells used for studies of "homozygous" WT and variant transporters were transfected with 200/67/20 ng WT or variant HA-EAAT2 cDNA/48w-well supplemented with "empty" pcDNA3.1 for a total of 200 ng cDNA/48w-well. Cells used for studies of "heterozygous" WT/variant transporters were either transfected with 100 ng variant HA-EAAT2 cDNA together with 100 ng WT EAAT2 cDNA or "empty" pcDNA3.1 per 48w-well, or transfected with 100/25 ng WT HA-EAAT2 cDNA together with 100/25 ng (untagged) WT EAAT2 cDNA, variant EAAT2 cDNA or "empty" pcDNA3.1 per 48w-well, supplemented with "empty" pcDNA3.1 for a total of 200 ng cDNA/48w-well.

On the day of the assay, cells were washed two times with ice-cold wash buffer (phosphate-buffered saline supplemented with 1 mM $CaCl_2$) and incubated in an ice-cold 4% paraformaldehyde solution for 12 min on ice, after which the following steps were performed at

room temperature. The cells were washed three times with wash buffer, incubated for 30 min in blocking solution (3% dry milk in 50 mM Tris-HCl, 1 mM $CaCl_2$, pH 7.5), and incubated with rat monoclonal anti-HA-peroxidase conjugated antibody (clone 3F10, Sigma–Aldrich (St. Louis, MO), diluted 1:1000 in blocking solution) for 1 h. Total expression levels of HA-tagged WT and variant EAAT2 in the cells were determined by adding 0.1% Triton X-100 in the blocking solution used for the blocking and the antibody incubation steps. Cells were then washed three times with washing buffer, and expression of the HA-tagged proteins was quantified using 3,3',5,5'-tetramethylbenzidine liquid substrate system (Sigma Aldrich) and H_2SO_4. The absorbance of the supernatants was determined at 450 nm. All experiments were performed in triplicate, and data are based on a total of three-four independent experiments.

[^{3}H]-D-Aspartate ([^{3}H]-D-Asp) uptake assay

The transport properties of WT and variant EAAT2 expressed in COS-7 cells were determined in a [^{3}H]-D-Asp uptake assay performed essentially as previously described.[45,46] Cells used for uptake studies of "homozygous" WT and variant transporters were transfected with 100 or 3.3 ng WT or variant EAAT2-mYFP-pRcCMV/46w-well, the latter condition supplemented with 96.7 ng "empty" pcDNA3.1 for a total of 100 ng cDNA/96w-well. Cells used for uptake studies of "heterozygous" WT/variant transporters were transfected with 50/5 ng WT EAAT2 cDNA together with 50/5 ng WT EAAT2 cDNA, variant EAAT2 cDNA, or "empty" pcDNA3.1 per 96w-well, supplemented with "empty" pcDNA3.1 for a total of 100 ng cDNA/96w-well.

On the day of the assay, the transfected cells in the 96-well plates were washed twice with 100 µL assay buffer (Hank's Buffered Saline Solution supplemented with 20 mM HEPES, 1 mM $CaCl_2$, and 1 mM $MgCl_2$, pH 7.4). Then 75 µL of assay buffer supplemented with 100 [^{3}H]-D-Asp (PerkinElmer, Boston, MA; specific activity: 16.5 Ci/mmol) in the absence or presence of various concentrations of D-Asp (in the D-Asp saturation uptake experiments, performed on both high- and low-expressing cells) or various concentrations of L-Glu, L-Asp and D-Asp (in the [^{3}H]-D-Asp uptake inhibition experiments, performed on high-expressing cells) were added to the wells, and the plate was incubated at 37 °C for 3 min. Nonspecific [^{3}H]-D-Asp uptake/binding in the cells was determined in the presence of 3 mM L-Glu. The assay mixtures were quickly removed from the wells, and the cells were washed twice with 100 µL ice-cold assay buffer, after which 150 µL Microscint-20 scintillation fluid (PerkinElmer) was added to each well. The 96-well plate was then shaken for at least 1 h and then counted in a TopCounter (PerkinElmer). The exact molar concentration of [^{3}H]-D-Asp in the "100 nM [^{3}H]-D-Asp"-solution was determined by counting in the TriCarb scintillation counter. All data are based on at least three independent experiments performed in duplicate.

Electrophysiology

Whole-cell patch clamp recording was performed using an EPC-10 amplifier (HEKA Elektronik, Goettingen, Germany) as previously described.[24] Transfected single HEK293T cells were clamped either to 0 mV or to –70 mV for at least 5 s between test sweeps, with an *a priori* junction potential correction. The standard bath solution contained (in mM): 140 $NaNO_3$, 4 KCl, 2 $CaCl_2$, 1 $MgCl_2$, 5 TEA, 10 HEPES, ±0.5 Na-L-Glu, pH 7.4, and the standard pipette solution contained (in mM): 115 KNO_3, 2 $MgCl_2$, 5 TEA-Cl, 5 EGTA, 10 HEPES, pH 7.4. Reversal potentials were measured under biionic conditions with external 140 NaCl and internal 115 Na-L-Glu or K-L-Glu, with cells held at –70 mV between sweeps. To quantify electrogenic transport currents, EAAT2 anion currents were abolished by substituting permeable anions, such as NO_3^- and Cl^-, by gluconate$^-$ (in mM), external: 140 Na-gluc, 4 K-gluc, 1 Mg-gluc, 2 Ca-gluc, 5 TEA, 10 HEPES ± 0.5 L-Glu, pH 7.4; internal: 115 K-gluc, 2 Mg-gluc, 5 EGTA, 10 HEPES, pH 7.4.

Data analysis and statistical methods

ELISA and [^{3}H]-D-Asp uptake data was analysed with GraphPad Prism 10.0 (GraphPad Software). Specific HA-EAAT2 expression and specific [^{3}H]-D-Asp uptake was determined by subtraction of values determined at mock-transfected cells in parallel. For the D-Asp saturation uptake experiments, specific D-Asp uptake in wells incubated with assay buffer containing 100 [^{3}H]-D-Asp and various concentrations of "cold" D-Asp was calculated by use of the specific activity for [^{3}H]-D-Asp and the dilution factor $C_{[3H]\text{-}D\text{-}Asp}/(C_{[3H]\text{-}D\text{-}Asp\ +\ D\text{-}Asp})$ determined by the specific [^{3}H]-D-Asp and "cold" D-Asp concentrations applied in the specific wells, a mathematical conversion that is based on the reasonable assumption that [^{3}H]-D-Asp and D-Asp possess identical properties as EAAT2 substrates. Specific D-Asp uptake data was fitted to one site-specific ligand binding model, and Michaelis transport constant (K_m) and maximal transport rate (V_{max}) values were determined by nonlinear regression. Concentration-inhibition data from the uptake assay was analysed with a nonlinear regression one site-fit log IC_{50} model, and inhibitor constants (K_i) were calculated using the "functional equivalent" of the Cheng–Prusoff equation.[47] Statistical analysis of ELISA and [^{3}H]-D-Asp uptake data was performed using *one-way* ANOVA followed up by Tukeys multiple comparisons post hoc test. In all tests significant differences of EAAT2 variants to WT are indicated by asterisks '*', with significance levels $*P \leq 0.05$/$**P \leq 0.01$/$***P \leq 0.001$/$****P \leq 0.0001$.

Electrophysiology data were analysed with Patchmaster Next (Multichannelsystems GmbH) and OriginPro 2020 (OriginLab). Current-voltage relationships

were constructed by plotting macroscopic current amplitudes determined during the last 10 ms of the voltage step vs. membrane potential. Mean fluorescence from WT-mCherry (defined as integrated fluorescence of the whole cell divided by its area) were measured with an Olympus IX-73 microscope equipped with a 64× objective and an Andor SCMOS camera[48] in combination with Fiji Image analysis software.[43] To examine a possible interaction between WT and variants, fluorescence to current ratios were fitted with a single linear originating at zero. Non-overlapping 95%-confidence areas of the fits indicate significant changes in these ratios. All data are given as means ± 95% confidence intervals (*C.I.*), unless otherwise stated. For statistical analysis of data, *one-way* ANOVA were used with Holm-Sidak *post hoc* tests or in single cases of single comparisons a *paired-t*-test or a Mann–Whitney *U* test. Normality of data was verified with Shapiro–Wilk tests. In all tests significant differences of EAAT2 variants to WT are indicated by asterisks '*', with significance levels $*P \leq 0.05/**P \leq 0.01/***P \leq 0.001/****P \leq 0.0001$.

Ethics

The study was conducted according to the ethical principles for medical research outlined in the Declaration of Helsinki. The study was approved by the Danish Health Research Ethics Committee in the Zealand region of Denmark (project number SJ-91). All probands or parents/legal guardians provided consent to participate in the study.

Role of funders

The funders had no role in study design, data collection, data analysis, interpretation or writing of the report.

Results

Genetic analysis

The 13 *SLC1A2* variants harboured by the 18 individuals in our cohort encompass heterozygous missense (10) and protein-truncating (1) variants and homozygous missense (1) and splice-site (1) variants (Fig. 1a). Variants occurred *de novo* in 11 individuals, including a monozygotic twin pair, or segregated with the disease in one family. The inheritance mode was unknown in the remaining three individuals with heterozygous variants. The remaining seven individuals harboured four previously published variants.[27–31]

The locations of the 13 variants in the EAAT2 protein are given in Fig. 1b–d. Three of the nine novel variants encode for amino acid exchanges in the amino- or carboxy-terminal regions of EAAT2 (p.Leu37Pro, p.His542Arg, p.Ile546Thr). Five other novel variants are located in TM2 (p.Leu85Arg), TM5 (p.Ile276Ser), HP1 (p.Gly360Ala) or HP2 (p.Ala432Asp, p.Ala439Val) of EAAT2, and the frameshift variant p.Phe249Serfs*17 produces a premature STOP codon 17 codons downstream of TM4c residue 249. This subset of the 9 novel missense variants (out of the total of 13 variants) were characterized functionally in this study. The other four variants—three variants located in TM2 (p.Gly82Arg,[27–29] p.Leu85Pro[29,30]) and TM5 (p.Pro289Arg[28]) and the splice-site variant c.1421+1G>C[31] that deletes exon IX and encodes a truncated EAAT2 with a novel STOP codon at position 474 in TM8—have all been functionally characterized previously.[24,31] Whereas G82R, L85P/L85R, P289R, A432D, A439V and c.1421+1G>C all reside in highly conserved regions across the EAATs, the remaining six missense variants affect less conserved residues (Fig. 1e).

Nine variants were classified as pathogenic or likely pathogenic according to ACMG guidelines, whereas the remaining four (p.Leu37Pro, p.Gly360Ala, p.His542Arg and p.Ile546Thr) were classified as variants of uncertain significance (VUS). All had CADD[37] scores between 24.5 and 36. Nine variants were absent in gnomAD v4.0, whereas p.Ala432Asp, p.Gly360Ala and p.Ile546Thr were present one or two times, and the homozygous variant p.Ala439Val was present six times in heterozygous state.

Subcellular distribution and expression properties of the EAAT2 variants

Since disease-causing missense variants can alter overall expression levels and/or the cellular trafficking of plasma membrane-expressed proteins, the impact of the 9 novel *SLC1A2* variants (8 missense variants and the truncation variant F249Sfs*17) on EAAT2 expression was investigated (Figs. 2 and 3). The subcellular distributions of YFP-fused WT and variant EAAT2 in HEK293T cells were studied by confocal microscopy imaging (Fig. 2a). WT EAAT2 displayed almost exclusive surface membrane insertion,[41] and introduction of L37P, I276S, G360A, A439V, H542R or I546T in the transporter did not impair its surface trafficking. In contrast, L85R, A432D and F249Sfs*17 were mainly expressed in intracellular compartments (Fig. 2a). We also determined total and cell surface expression levels of extracellularly HA-tagged WT and variant EAAT2 in COS-7 cells transfected with three different cDNA quantities in an ELISA, thus quantifying transporter expression levels in their dynamic ranges (Fig. 3a). L85R, A432D and F249Sfs*17 exhibited pronouncedly reduced total and cell surface expression levels compared to WT EAAT2, and a trend of lower total and cell surface expression of I276S compared to the WT transporter was also observed. In contrast, G360A, A439V and I546T exhibited statistically significant higher total and cell surface expression levels than WT EAAT2 at some of the three transfection levels, whereas L37P and H542R displayed WT-like expression properties (Fig. 3a).

While the expression properties displayed by the variants expressed as "homozygous" transporters in

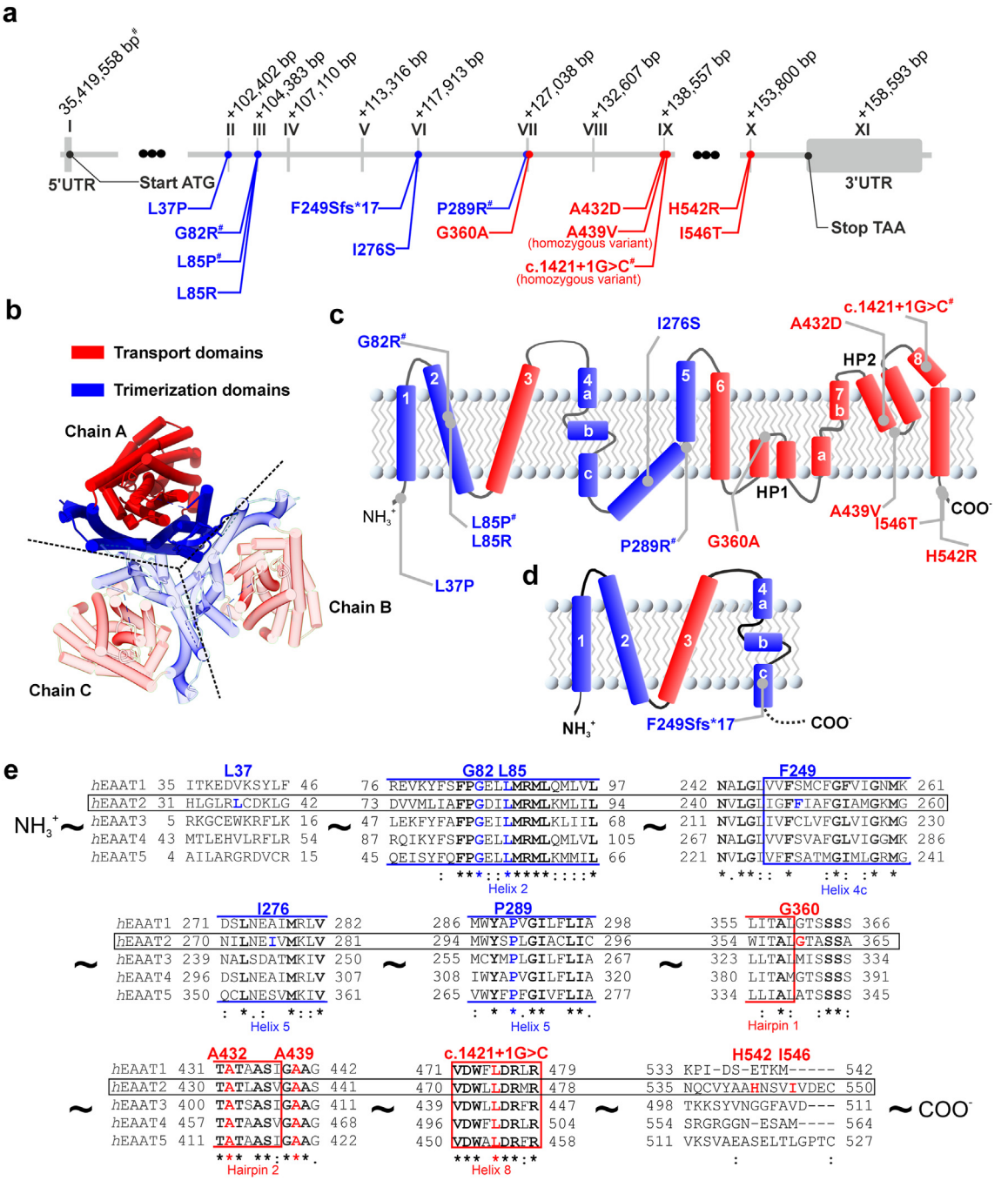

Fig. 1: **Gene structure of *SLC1A2* and the positions of the *SLC1A2* missense variants in the EAAT2 protein.** (**a**) Genomic assembly of *SLC1A2* with positions of missense base exchanges within exons (I-XI). The gene structure was extracted from *SLC1A2* sequence information by *ensemble.org* (GRCh38.p14, ENST00000278379.9). Base pair numbering indicates starting regions of exons downstream to the gene starting site (denoted as #). (**b**) Extracellular view of the 3-dimensional structure of the EAAT2 trimer derived from pdb structure 7XR4 (www.rcsb.org).[49,50] The dashed lines indicate the limits for each monomer. (**c, d**) 2-dimensional transmembrane topologies of the fully (**c**) or truncated (**d**) EAAT2 monomers with indicated positions of the *SLC1A2* missense variants. Regions forming the trimerization and the transport domains in the EAAT2 monomer are shown in blue and red, respectively. Multiple sequence alignment of stretches from the five human EAAT subtypes covering the nearest amino acid residues surrounding the mutated residues in sequential order. Regions within helices are highlighted by colour, as in b and c. Conserved residues are given in bold and indicated with asterisks. (**a, c**) Variants that were functionally characterized in previous studies[24,29–31] are indicated with a hash.

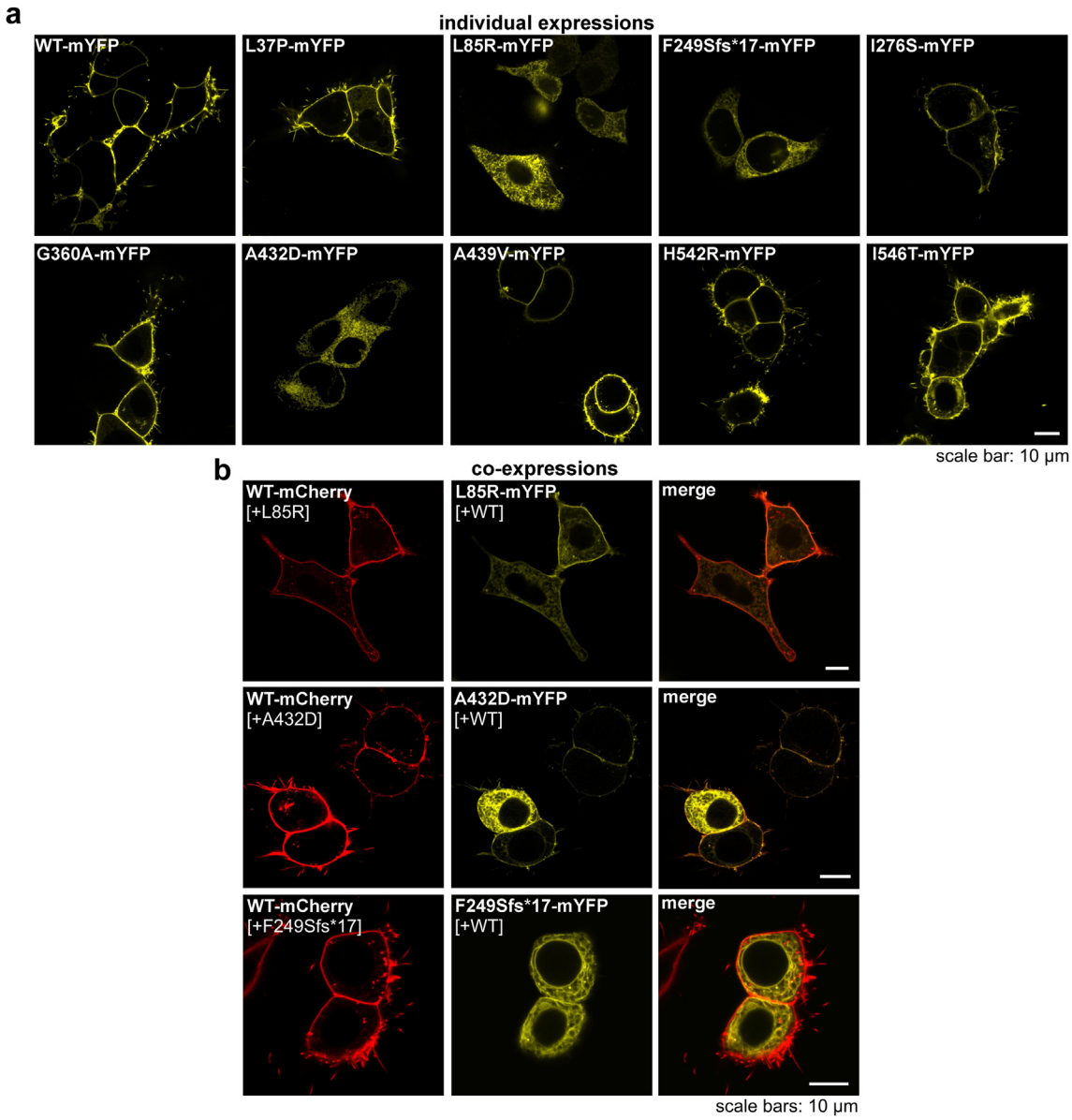

Fig. 2: **Expression properties exhibited by WT EAAT2 and nine EAAT2 variants in confocal microscopy.** (**a**) Representative confocal microscopy images of HEK293T cells expressing WT or variant EAAT2 fused to mYFP. (**b**) Confocal microscopy images of HEK293T cells co-expressing WT EAAT2 fused to mCherry and variants L85R-mYFP, A432D-mYFP or F249Sfs*17-mYFP.

the HEK293T and COS-7 cells are informative, most of the variants in this study are heterozygous and thus potentially capable of assembling into WT/variant EAAT2 heterotrimers in the heterozygous individual. Although the monomers in the EAAT trimer operate largely independently both in terms of their transport and anion conductance.[5,51–53] the variants could modify overall EAAT2 function by changing the intracellular trafficking, the membrane turnover, and/or the lifespan of these heterotrimeric transporters compared to WT EAAT2. Thus, we also studied the expression properties of the three variants characterized by dramatically reduced membrane insertion (L85R, F249Sfs*17 and A432D) when these were co-expressed with WT EAAT2 in HEK293T or COS-7 cells. Whereas co-expression of F249Sfs*17 with WT EAAT2 had no effect on total or cell surface expression levels of this truncated variant, surface expression levels of both A432D and L85R were significantly increased in cells co-expressing WT EAAT2 compared to those of the individual variants expressed

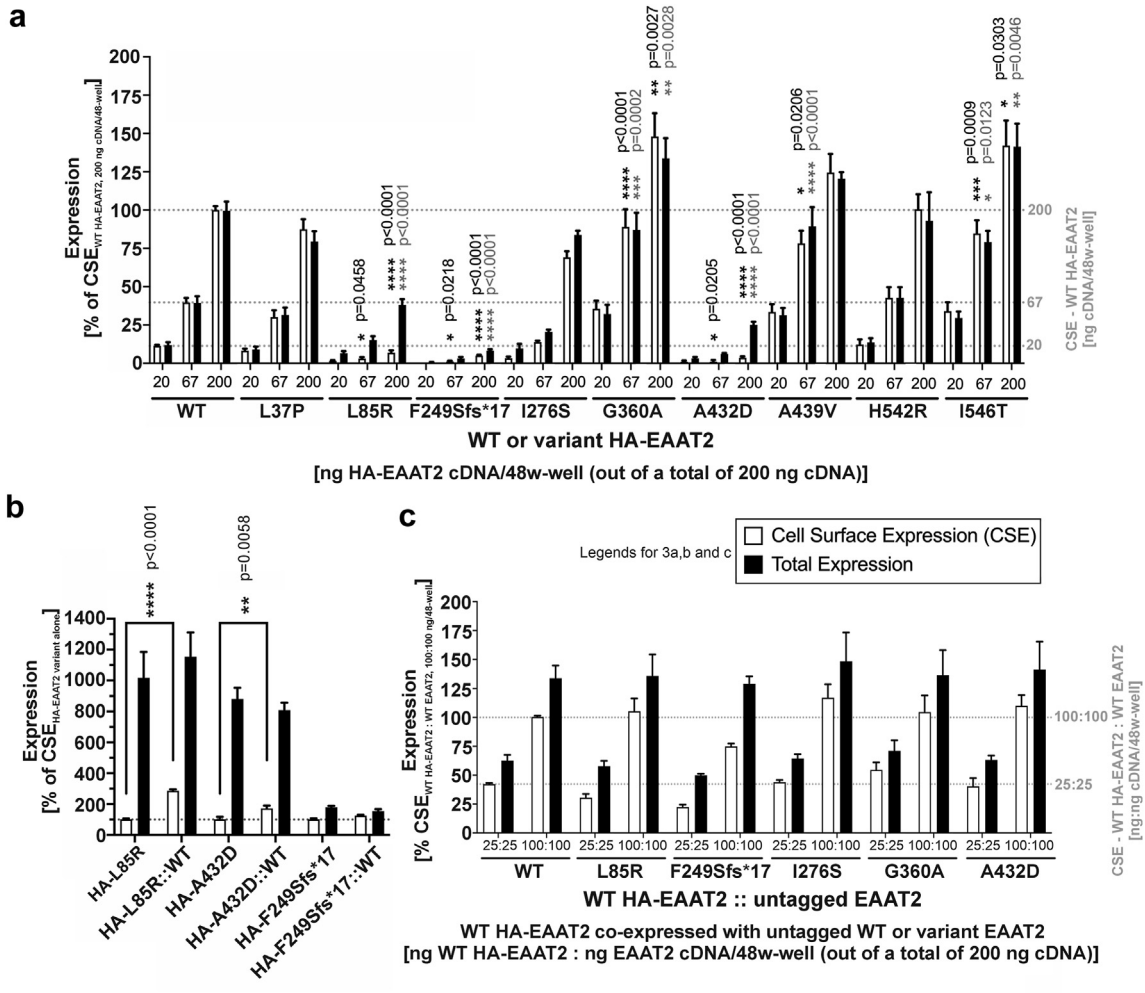

Fig. 3: **Expression properties exhibited by WT EAAT2 and nine EAAT2 variants in an ELISA.** Cell surface and total expression levels displayed by HA-tagged versions of WT and variant EAAT2 transiently expressed in COS-7 cells in an ELISA. (**a**) Expression levels displayed by HA-tagged WT and variant EAAT2 in cells transfected with three different cDNA amounts (20, 67 and 200 ng EAAT2 cDNA of a total cDNA quantity of 200 ng per 48w-well). Data are given as mean ± S.E.M. in % of the cell surface expression level of WT HA-EAAT2 (200 ng cDNA/48w-well) and are based on three independent experiments (n = 3) performed in triplicate. The mean cell surface expression levels of WT HA-EAAT2 at the three different cDNA transfection levels are indicated with grey hatched lines. Statistically significant differences between WT HA-EAAT2 vs. variant HA-EAAT2 expression at each of the three different transfection levels are indicated (black for cell surface expression, grey for total expression). (**b**) Expression levels displayed by HA-tagged L85R, A432D and F249Sfs*17 EAAT2 expressed in cells on their own (100 ng variant HA-EAAT2 cDNA and 100 ng "empty" pCDNA3.1 per 48w-well) or together with (untagged) WT EAAT2 (100 ng variant HA-EAAT2 cDNA and 100 ng WT EAAT2 cDNA per 48w-well). Data are given as mean ± S.E.M. in % of the cell surface expression level of the HA-tagged variant on its own (indicated with a grey hatched line) and are based on three independent experiments (n = 3) performed in triplicate. Statistically significant differences between HA-EAAT2 variant expression on its own vs. co-expressed with untagged WT EAAT2 are indicated. (**c**) Expression levels displayed by HA-tagged WT EAAT2 co-expressed with untagged WT or variant EAAT2 in cells transfected with two different cDNA amounts (25:25 ng and 100:100 ng WT HA-EAAT2:untagged EAAT2 cDNA of a total cDNA quantity of 200 ng per 48w-well). Data are given as mean ± S.E.M. in % of the cell surface expression level of WT HA-EAAT2 co-expressed with WT EAAT2 (100 ng:100 ng cDNA/48w-well) and are based on four independent experiments (n = 4) performed in triplicate. The mean cell surface expression levels of WT HA-EAAT2 co-expressed with untagged WT EAAT2 at the two different cDNA transfection levels are indicated with grey hatched lines. Statistical analysis did not identify any statistically significant differences between WT HA-EAAT2 expression when co-expressed with WT EAAT2 vs. when co-expressed with variant EAAT2. (**a–c**) Statistical analyses were performed using *one-way* ANOVA followed up by Tukeys multiple comparisons *post hoc* test. All statistically significant differences are indicated by asterisks and P values, with significance levels: $^{*}P \leq 0.05$/$^{**}P \leq 0.01$/$^{***}P \leq 0.001$/$^{****}P \leq 0.0001$.

alone (Figs. 2 and 3b). However, cell surface expression levels displayed by these two variants in the presence of WT EAAT2 were still very modest compared to that of WT EAAT2 itself (Fig. 3a and b), indicating substantially lower overall EAAT2 surface expression levels in individuals harbouring these variants.

As the presence of the EAAT2 variant conversely also could impact WT EAAT2 expression properties in the cells of the heterozygous carrier, we also probed the putative impact of the five heterozygous variants that displayed distinct expression and/or functional properties compared to WT EAAT2 on the expression properties of the WT transporter. This was done in ELISA experiments on COS-7 cells co-transfected with HA-tagged WT EAAT2 and untagged WT or variant EAAT2 in 1:1 cDNA ratios at two different cDNA quantities (Fig. 3c). Here the total and cell surface expression levels exhibited by WT HA-EAAT2 in cells co-expressing either of these five variants were found not to be statistically significant different from those in the control HA-WT::WT-transfected cells, albeit a tendency to reduced WT HA-EAAT2 cell surface expression levels was observed for the HA-WT::F249Sfs*17 combination (Fig. 3c).

Transport properties of the EAAT2 variants

The putative changes in EAAT2 transport function induced by the nine novel *SLC1A2* variants were investigated in a [^{3}H]-D-Asp uptake assay (Fig. 4).[45,46] Importantly, we both investigated transport properties in COS-7 cells transfected with high and low EAAT2 cDNA quantities and our findings were very similar in these high- and low-expressing cells (Table 1). L37P, G360A, H542R and I546T all displayed maximum uptake capacities (D-Asp V_{max}) not significantly different from the D-Asp V_{max} of WT EAAT2 (Table 1, Fig. 4a). In contrast, no significant [^{3}H]-D-Asp uptake was detectable in COS-7 cells transfected with A432D or F249Sfs*17, and only very small [^{3}H]-D-Asp uptake levels were detected in cells transfected with high L85R EAAT2 cDNA quantities (Table 1). I276S displayed a moderately reduced D-Asp V_{max} compared to WT EAAT2, probably because of its modestly reduced surface expression levels compared to the WT transporter (Table 1, Figs. 3a and 4a). Interestingly, A439V exhibited a markedly lower D-Asp V_{max} than WT EAAT2 even through this variant displayed comparable cell surface expression levels compared to the WT transporter (Table 1, Figs. 3a and 4a). A correlation analysis of the D-Asp V_{max} values and cell surface expression levels of the transporters shows that the maximal transport capacities of L37P, L85R, I276S, and H542R correlate well with their respective cell surface expression levels (R^2_{corr} = 0.9431, Fig. 4b). G360A and I546T both displayed WT-like V_{max} values, even though the cell surface expression levels of these two variants were somewhat higher than that of the WT transporter. Most notably, however, the WT-like cell surface expression observed for A439V was contrasted by its dramatically decreased transport capacity, and thus this variant stood out as a well expressed but truly functionally compromised transporter (Fig. 4b).

The D-Asp K_m values determined for L37P, I276S, G360A, H542R and I546T did not differ significantly from that at WT EAAT2 in the saturation uptake experiments, and D-Asp and L-Glu both displayed comparable K_i values in their inhibition of [^{3}H]-D-Asp uptake through WT and these five variants (Fig. 4a and c, Table 1). In contrast, D-Asp exhibited 9- and 14-fold lower K_m and K_i values at A439V than at WT EAAT2, respectively, and the K_i of L-aspartate (L-Asp) was 11-fold lower at A439V than at the WT transporter (Fig. 4a and c, Table 1 and table footnote). Notably, however, L-Glu displayed comparable K_i values at A439V and WT EAAT2 (Fig. 4c, Table 1). In concordance with this finding, an A440C mutation of the corresponding alanine residue in EAAT1 has been reported to yield markedly reduced transport capacity but no change in L-Glu K_m.[54] The differential effect of this variant on the EAAT2 substrate potencies is quite interesting from a molecular perspective. Considering the proximity of Ala^{439} to the substrate binding site in EAAT2, it is possible that this variant induces a structural change in this site that yields increased binding affinities of the shorter EAAT2 substrates (D-Asp and L-Asp) while not altering transporter binding of the longer substrate L-Glu. However, keeping the focus of this study in mind, the unchanged apparent substrate potency displayed by the major endogenous EAAT2 substrate L-Glu at A439V means that the molecular phenotype of this variant in terms of transport function is its markedly reduced transport capacity.

To approximate the EAAT2-mediated transport in the heterozygous individual harbouring WT and variant *SLC1A2* alleles, we next characterized the uptake properties in COS-7 cells transfected with combinations of WT and variant (L85R, F249Sfs*17, I276S, G360A or A432D) EAAT2 cDNAs in 1:1 ratios at two different cDNA quantities in the [^{3}H]-D-Asp uptake assay (Table 1, Fig. 4d). In these experiments, WT::WT-cells (cells transfected with double the amount of WT EAAT2 cDNA as the WT::variant combinations) and WT::vector-cells (cells transfected with WT EAAT2 and "empty" vector cDNA in a 1:1 ratio) served as the "homozygous" WT control and as the hypothetical "one WT-allele only" control assessing the uptake mediated by WT EAAT2 on its own, respectively. None of the D-Asp K_m values determined for the five "heterozygous" WT::variant combinations differed significantly from those of the WT::WT or WT::vector combinations, which was not surprising given that these variants when tested as "homozygous" transporters either exhibit WT-like K_m values (I276S, G360A) or display negligible cell surface expression (L85R, F249Sfs*17, A432D)

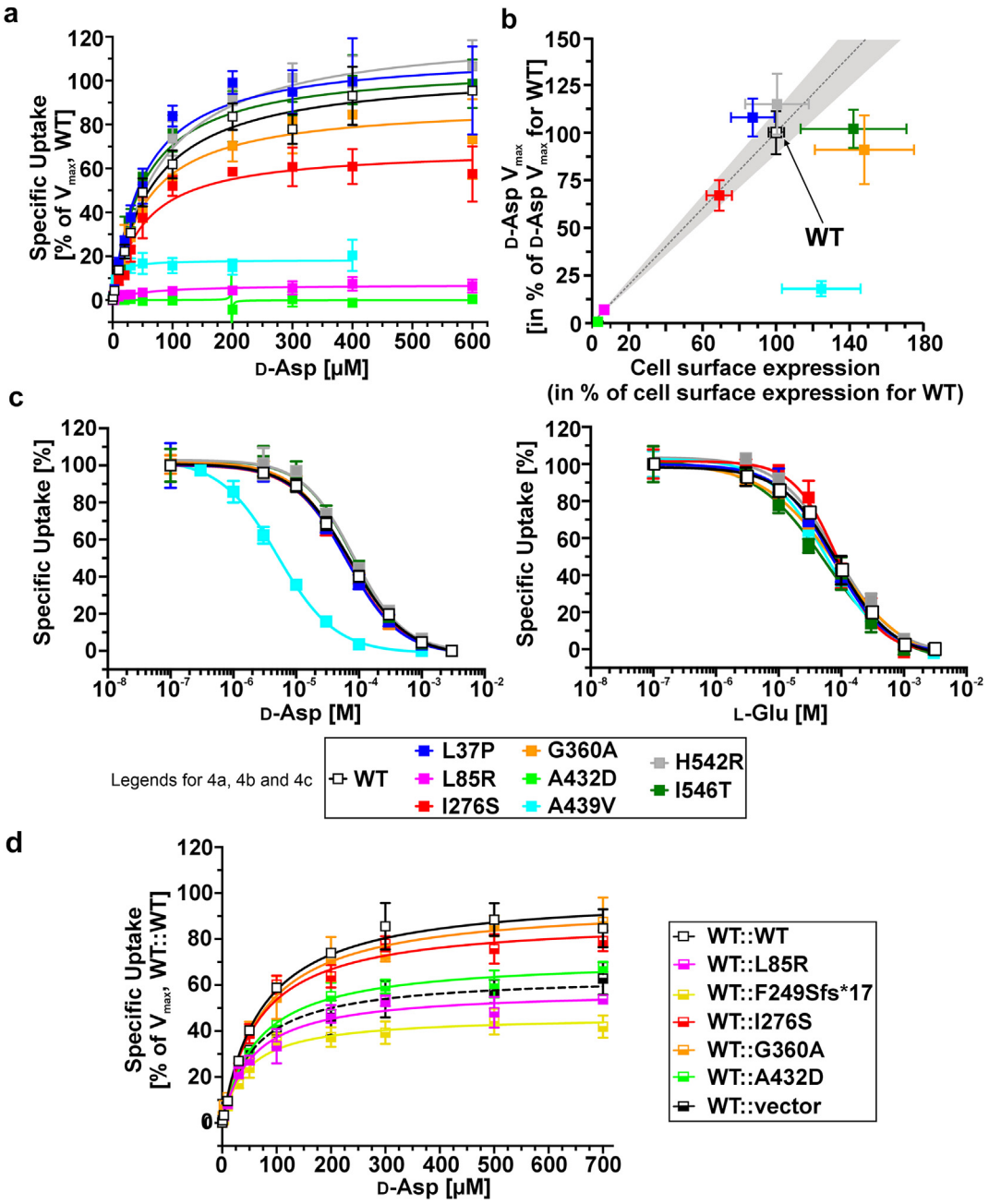

Fig. 4: **Transport properties exhibited by WT EAAT2 and nine EAAT2 variants.** The functional properties of WT and variant transporters fused to YFP transiently expressed in COS-7 cells were characterized in a [^{3}H]-D-Asp uptake assay. (**a**) Saturation D-Asp uptake exhibited by "homozygous" WT and variants in the [^{3}H]-D-Asp uptake assay in cells transfected with 100 ng EAAT2 cDNA/96w-well. Data are from representative individual experiments and are given as mean ± S.D. in % of the fitted V_{max} exhibited by WT EAAT2 on the same 96-well plate. The average K_m and V_{max} values for D-Asp at WT and variant EAAT2 are given in Table 1. (**b**) Plot of the D-Asp V_{max} values of "homozygous" WT and variant EAAT2 (mean ± S.D., normalized to WT EAAT2 D-Asp V_{max}, Table 1) against the cell surface expression levels of HA-tagged WT and variant EAAT2 (mean ± S.D., normalized to WT EAAT2 cell surface expression, Fig. 3a). The dashed line indicates the extrapolated mean values of D-Asp uptake starting from zero expression and the grey shaded area indicates the extrapolated S.D. for the uptake at every expression level. Data in the plot are from Table 1 and Fig. 3a. (**c**) Concentration-inhibition relationships exhibited by D-Asp (*left*) and L-Glu (*right*) at "homozygous" WT and variant EAAT2 in the [^{3}H]-D-Asp uptake assay. Data are from representative individual experiments and are given as means ± S.D. in % of the specific [^{3}H]-D-Asp uptake in the absence of test compound. The average K_i values for D-Asp and L-Glu in their competition inhibition of [^{3}H]-D-Asp uptake at WT and variant EAAT2 are given in Table 1. (**d**) Saturation D-Asp uptake exhibited by

"Homozygous" EAAT2	D-Asp saturation uptake				Competitive inhibition of [^{3}H]-D-Asp uptake	
	100 ng EAAT2 cDNA/96w-well		3.3 ng EAAT2 cDNA/96w-well		D-Aspartate	L-Glutamate
	K_m ± S.E.M.	V_{max} ± S.E.M.$^{(n)}$	K_m ± S.E.M	V_{max} ± S.E.M.$^{(n)}$	K_i [pK_i ± S.E.M.]$^{(n)}$	K_i [pK_i ± S.E.M.]$^{(n)}$
WT[c]	55 ± 6	100 ± 4$^{(8)}$	40 ± 3	100 ± 5$^{(6)}$	68 [4.17 ± 0.03]$^{(6)}$	85 [4.07 ± 0.04]$^{(6)}$
L37P	61 ± 4	108 ± 5$^{(4)}$	50 ± 7	113 ± 6$^{(3)}$	65 [4.19 ± 0.08]$^{(4)}$	78 [4.11 ± 0.05]$^{(4)}$
L85R	n.d.[b]	n.d.$^{(3)}$ [b]	no significant uptake$^{(3)}$ [a]		–[c]	–[c]
F249Sfs*17	no significant uptake$^{(3)}$ [a]		no significant uptake$^{(3)}$ [a]		–[c]	–[c]
I276S	56 ± 4	67 ± 4** P = 0.0019 (4)	35 ± 4	57 ± 7** P = 0.0019 (4)	69 [4.16 ± 0.05]$^{(4)}$	86 [4.07 ± 0.03]$^{(4)}$
G360A	54 ± 5	91 ± 9$^{(4)}$	46 ± 6	109 ± 11$^{(3)}$	55 [4.26 ± 0.06]$^{(4)}$	69 [4.16 ± 0.08]$^{(4)}$
A432D	no significant uptake$^{(3)}$ [a]		no significant uptake $^{(3)}$ [a]		–[c]	–[c]
A439V[e]	6.4 ± 1.3**** [d]	18 ± 2**** P < 0.0001 (4)	n.d.[b]	n.d.$^{(3)}$ [b]	4.7 [5.33 ± 0.09]**** [d] (4)	55 [4.24 ± 0.07]$^{(4)}$
H542R	73 ± 7	115 ± 8$^{(4)}$	29 ± 4	99 ± 8$^{(4)}$	66 [4.18 ± 0.07]$^{(4)}$	89 [4.05 ± 0.07]$^{(4)}$
I546T	58 ± 6	102 ± 5$^{(4)}$	46 ± 6	125 ± 6$^{(3)}$	77 [4.11 ± 0.03]$^{(4)}$	55 [4.26 ± 0.07]$^{(4)}$

"*Heterozygous*" EAAT2	D-Asp saturation uptake				
	WT:variant cDNA	50 ng WT EAAT2 : 50 ng EAAT2 cDNA/96w-well		5 ng WT EAAT2 : 5 ng EAAT2 cDNA/96w-well	
	(% of 100 ng/10 ng)	K_m ± S.E.M.	V_{max} ± S.E.M.$^{(n)}$	K_m ± S.E.M.	V_{max} ± S.E.M.$^{(n)}$
WT::WT	100::0	63 ± 6	100 ± 4$^{(6)}$	64 ± 5	100 ± 3$^{(6)}$
WT::L85R	50::50	55 ± 4	57 ± 4*** P = 0.0002 (4)	44 ± 5	54 ± 4**** P < 0.0001 (4)
WT::F249Sfs*17	50::50	48 ± 2	44 ± 2**** P < 0.0001 (4)	59 ± 6	43 ± 4**** P < 0.0001 (3)
WT::I276S	50::50	74 ± 6	91 ± 9# P = 0.0376 (4)	50 ± 2	83 ± 6# P = 0.0118 (4)
WT::G360A	50::50	67 ± 9	90 ± 9# P = 0.0487 (4)	62 ± 8	91 ± 6### P = 0.0007 (4)
WT::A432D	50::50	69 ± 7	71 ± 3* P = 0.0137 (4)	66 ± 8	69 ± 3*** P = 0.0007 (4)
WT::vector	50::0	68 ± 8	63 ± 6** P = 0.0011 (4)	48 ± 5	57 ± 6**** P < 0.0001 (4)

Top section of table: *Functional properties of "homozygous" EAAT2 in cells expressing WT or variant transporters on their own.* Based on the D-Asp saturation uptake, D-Asp K_m (±S.E.M.) values are given in μM, and D-Asp V_{max} (±S.E.M.) values are given in % normalised to the V_{max} of WT EAAT2-expressing cells (100 ng or 3.3 ng WT EAAT2 cDNA/96w-well). Based on the competitive inhibition of [^{3}H]-D-Asp uptake, the D-Asp and L-Glu K_i values are given in μM (with pK_i ± S.E.M. in brackets). The numbers of individual experiments (n) for the data are given in superscript after the data. Statistical analysis was performed using *one-way* ANOVA followed up by Tukeys multiple comparisons post hoc test. Significant differences of EAAT2 variant values to WT EAAT2 values are indicated by asterisks and *P* values (with significance levels $^{**}P \leq 0.01$/$^{****}P \leq 0.0001$). ***Bottom section of table:*** *Functional properties of "heterozygous" EAAT2 in cells co-expressing WT and variant transporters.* Based on the D-Asp saturation uptake, D-Asp K_m (±S.E.M.) values are given in μM, and D-Asp V_{max} (±S.E.M.) values are given in % normalised to the V_{max} of WT::WT EAAT2-expressing cells (100 ng or 10 ng WT EAAT2 cDNA/96w-well). The numbers of individual experiments (n) for the data are given in superscript after the data. Statistical analysis was performed using *one-way* ANOVA followed up by Tukeys multiple comparisons post hoc test. Significant differences of WT::variant and WT::vector values to WT::WT values are indicated by asterisks and *P* values (with significance levels $^{*}P \leq 0.05$/$^{**}P \leq 0.01$/$^{***}P \leq 0.001$/$^{****}P \leq 0.0001$), and significant differences of WT::variant values to WT::vector values are indicated by hash tags and *P* values (with significance levels $^{\#}P \leq 0.05$/$^{\#\#\#}P \leq 0.001$). [a]The [^{3}H]-D-Asp uptake measured in these cells using radiosubstrate concentrations up to 300 nM was not significantly different from that in mock-transfected cells. [b]n.d., not determinable. Significant but very minute levels of [^{3}H]-D-Asp uptake was detected, and thus K_m and V_{max} values could not be determined accurately. [c]Because of the lack of or very minute levels of [^{3}H]-D-Asp uptake measured in L85R-, F249Sfs*17- and A432D-transfected cells, competition inhibition experiments could not be performed for these mutants. [d]$^{****}P < 0.0001$. [e]The competitive inhibition of [^{3}H]-D-Asp uptake through at WT and A439V EAAT2 mediated by L-Aspartate was also determined: L-Aspartate K_i [pK_i ± S.E.M.]: 56 μM [4.31 ± 0.06] (WT) vs. 4.5 μM [5.37 ± 0.10] (A439V), n = 3 for both, ($^{**}P$ = 0.0025, *two-tailed* t-test).

Table 1: **Functional properties exhibited by WT and variant EAAT2 in COS-7 cells in the [^{3}H]-D-Asp uptake assay.**

(Fig. 4a and d, Table 1). Notably, however, at both cDNA transfection levels the five WT::variant combinations grouped into two distinct groups in terms of their maximum uptake capacities (D-Asp V_{max}). The V_{max} values determined in WT::I276S- and WT::G360A-expressing cells did not differ significantly from the V_{max} for the "homozygous" WT::WT combination but were significantly higher than the V_{max} in WT::vector-transfected cells. Conversely, the V_{max} values exhibited by the transporters in WT::L85R-, WT::F249Sfs*17- and WT::A432D-cells were all significantly lower than V_{max} for the "homozygous" WT::WT combination but not significantly different from the V_{max} for WT::vector-transfected cells (Fig. 4d, Table 1). A tendency to lower V_{max} values for WT::F249Sfs*17 compared to WT::vector-cells was observed (Fig. 4d, Table 1), which parallels the somewhat lower cell surface expression levels exhibited by the WT transporter in cells co-expressing this truncation variant (Fig. 3c). However, neither of these differences observed for WT::F249Sfs*17-cells were statistically significant.

"heterozygous" WT/variant EAAT2 combinations in the [^{3}H]-D-Asp uptake assay in cells (co-transfected with 50 ng WT EAAT2 cDNA and 50 ng WT or variant EAAT2 cDNA per 96w-well). Data for the WT::WT (100 ng WT EAAT2 cDNA/96w-well; open squares, *black solid line*) and WT:vector (50 ng WT EAAT2 cDNA/96w-well; full/open squares, *black dashed line*) controls are included. Data are from a representative individual experiment and are given as mean ± S.D. in % of the fitted V_{max} exhibited by "homozygous" WT EAAT2 (100 ng cDNA/96-w well). The average K_m and V_{max} values for D-Asp at the various combinations are given in Table 1.

EAAT2 L-Glu transport is electrogenic and can thus be studied in individual cells by whole-cell patch clamp recordings. This allows the comparison of L-Glu uptake in cells that differ in the relative expression of WT and mutant transporters as an alternative approach to test for possible functional interactions of mutant subunits with WT. We therefore analysed the L-Glu transport currents in HEK293T cells co-expressing WT EAAT2 and each of the variants L85R, F249Sfs*17 and A432D by whole-cell patch clamp recordings. Mutant EAAT2 was fused to mYFP and WT to mCherry, and cells were co-transfected at 1:1 cDNA ratios. To separate EAAT2 L-Glu currents from anion currents, permeant anions in internal and external solutions are usually substituted with gluconate, which is too large to pass through the EAAT2 anion channel.[11,55,56] This approach was not possible for L85R, since this variant renders the EAAT2 anion channel permeable to gluconate (see below).

Supplementary Fig. S1 depicts transport current densities from WT EAAT2-mCherry. At −125 mV, we obtained a mean current density was −7.3 ± 1.3 pA/pF (n = 14), closely similar to recently published values for WT EAAT2-mYFP (−6.1 ± 1.8 pA/pF, Supplementary Fig. S1b, calculated from freely available data: https://github.com/peterkovermann/epileptic_encephalopathy_1).[24] Co-expression of F249Sfs*17 or A432D with WT EAAT2 reduced current densities by about 50% (Mean ± *C.I.* at −125 mV: WT::F249Sfs*17: −3.7 ± 1.6 pA/pF, WT::A432D: n = 11/11, Supplementary Fig. S1b–d). Plots of L-Glu transport currents vs. whole-cell mCherry fluorescence amplitudes illustrate the two distinct mechanisms, by which the two variants reduce L-Glu transport. Co-expression of F249Sfs*17 EAAT2 reduced mCherry fluorescence amplitude, while—at identical mCherry fluorescence—the transport currents remain comparable (Supplementary Fig. S1c). In cells co-expressing WT and A432D EAAT2, mCherry fluorescence amplitudes were comparable with cells expressing WT EAAT2 alone, however, fluorescence to current ratios were significantly reduced (Supplementary Fig. S1c).

Anion channel properties of the EAAT2 variants

We studied anion conduction by WT and mutant EAAT2 in whole-cell patch clamp recordings in HEK293T cells. F249Sfs*17 was excluded from this analysis because of its exclusive intracellular localization. In these experiments, NO_3^- was used as predominant intra- and extracellular anion. EAAT2 Cl^- current amplitudes are small,[11,56] but increased above transport current amplitudes by larger and polyatomic anions (Supplementary Fig. S2). Since NO_3^- currents are 8-fold larger than transport currents, NO_3^- allows for easy separation of anion and transport currents without pharmacological subtraction procedures.[20]

Variants causing robust gain-of-anion-channel or loss-of-anion-channel function

The anion channel properties of WT EAAT2 and of the three mutants characterized by markedly impaired surface expression and/or transport function, L85R, A432D and A439V, are given in Fig. 5. In absence of external L-Glu, anion currents were comparable for WT, L85R and A439V EAAT2. Addition of L-Glu pronouncedly increased WT EAAT2 anion currents, but inhibited L85R anion currents. Thus, the L85R variant not only dramatically reduced EAAT2 cell surface expression but also changed its anion channel function. In contrast, the A439V mutation that increases EAAT2 cell surface expression was found to abolish channel-mediated anion currents (Fig. 5a–d).

Since A432D eliminated EAAT2 surface membrane insertion (Fig. 2a and 3a), we did not study this variant when expressed alone. In cells co-expressing A432D and WT EAAT2, NO_3^- current densities in the absence of L-Glu were increased compared to WT EAAT2-expressing cells (P = 0.0003, *two-tailed t-test*). L-Glu activated WT::A432D anion channels to a smaller degree than the WT anion channels (Fig. 5a–d). In cells co-expressing WT and L85R, we observed large inwardly rectifying anion currents in the absence of L-Glu, with ~28-fold larger amplitudes than cells expressing L85R alone. L-Glu inhibited these currents to levels slightly above those recorded from WT EAAT2-expressing cells (Fig. 5a–d). In symmetrical Cl^-, WT::L85R-mediated currents (Mean ± *C.I.*, without L-Glu: 228.2 ± 76.1/ n = 11) were comparable to those from cells expressing L85P EAAT2 (with L-Glu: 247 ± 74.8 pA·pF^{-1}) (Supplementary Fig. S3), however addition of L-Glu caused current inhibition in L85R (WT::L85R, mean ± *C.I.*, with L-Glu: −135.3 ± 38.6 pA·pF^{-1}, n = 11).

We recently demonstrated that L85P makes the EAAT2 anion channel permeable to L-Glu and L-gluconate.[24] To test for L-gluconate permeation through L85R anion channels, cells co-expressing WT and L85R EAAT2 were intracellularly dialysed with K-gluconate-based solutions and externally perfused Na-gluconate-based solutions (Fig. 6a and b). Whereas WT EAAT2 alone do not generate any currents under these conditions, cells additionally expressing WT::L85R-cells exhibited robust currents over the whole tested voltage range (Fig. 6a and b). In other experiments, where cells were internally dialysed with L-Glu-based solutions and external perfused with Cl^- (140 mM), we also observed large currents in both directions, whereas no currents at negative potentials indicative of L-Glu flux out of the cell was observed in the WT EAAT2-cells under these experimental conditions (Fig. 6c and d). Since these experiments were performed under conditions that prevent secondary-active L-Glu transport, i.e., no L-Glu (Fig. 6a and b) or no K^+ (Fig. 6c and d) in the external solution, these results indicate that L85R renders the EAAT2 anion channel permeant to gluconate and L-Glu.

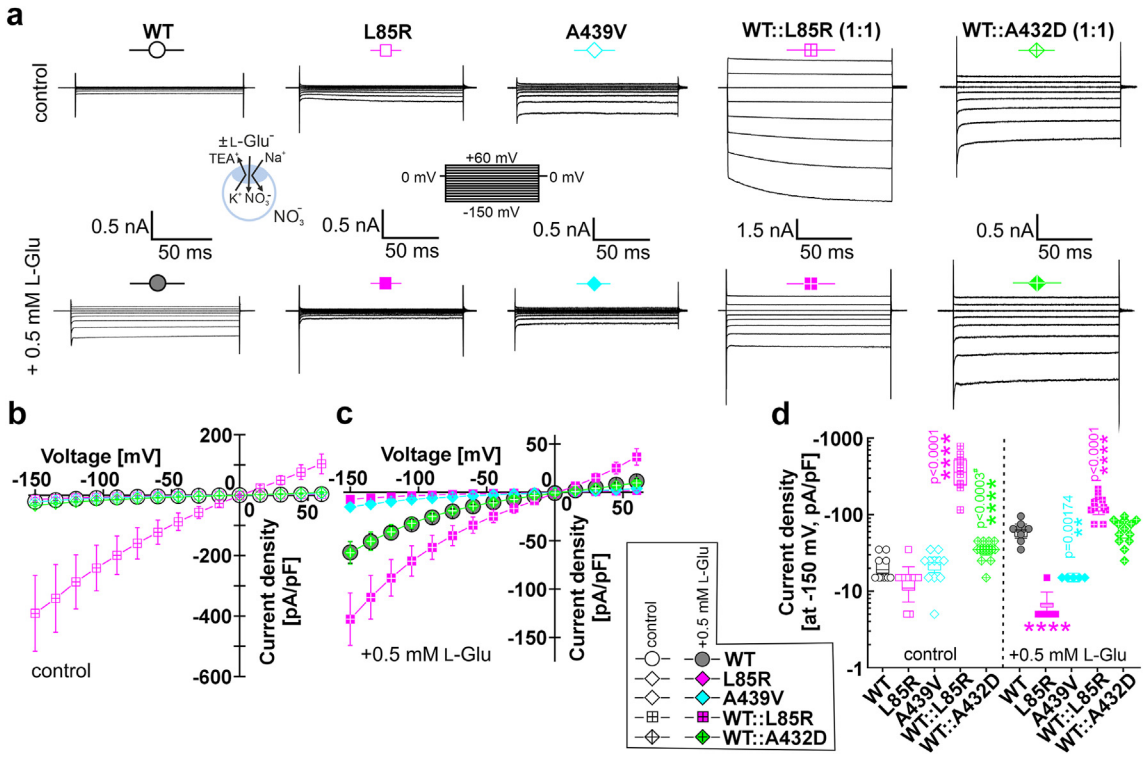

Fig. 5: **L85R, A432D and A439V EAAT2 variants cause loss-of-anion-channel or robust gain-of-anion-channel function.** (**a**) Representative whole-cell patch clamp recordings from HEK293T cells expressing WT, L85R or A439V EAAT2 and from cells co-expressing WT with L85R or A432D EAAT2 (WT::L85R, WT::A432D, 1:1 cDNA ratios) in the absence (control, *top*) or in the presence of 0.5 mM L -Glu (*bottom*). (**b, c**) Mean whole-cell current-voltage relationships in the absence (**b**) or presence (**c**) of 0.5 mM L-Glu (−150 mV: WT: wo L-Glu: −21.4 ± 4, with L-Glu: −62.1 ± 11.1 pA·pF^{-1}, *n* = 10/9; L85R: wo L-Glu: −14 ± 5.8; with L-Glu: −7.2 ± 2.1 pA·pF^{-1}, *n* = 9/8; A439V: wo L-Glu: −22.6 ± 4.6, with L-Glu: −15.2 ± 1.4 pA·pF^{-1}, *n* = 11/5; WT::L85R: (−150 mV: wo L-Glu: −390.8 ± 125.2, with L-Glu: 131.1 ± 27, pA·pF^{-1}, *n* = 10/10); WT::A432D: wo L-Glu −33.9 ± 3.9; with L-Glu: −62,4 ± 11,8 pA·pF^{-1}, *n* = 14/13). (**d**) Statistical analysis of whole cell current densities at −150 mV for WT and variants using *one-way* ANOVAs for each condition and Holm-Sidak *post hoc* testing (#the value for comparison of WT to WT::A432D is shown for a single comparison with a *two-sample two-tailed t-test with* $P = 2.92743 \times 10^{-4}$). Box plots show upper and lower quartiles with data medians and all error bars and whiskers span 95% confidence intervals of current amplitudes.

Variants causing mild gain-of-anion-channel function or without measurable effect on anion channel function

The G360A and I276S variants both increased anion current amplitudes compared to WT EAAT2 (Fig. 7). Thus, both variants induce mild gain-of-anion-channel activity in the transporter, in the case of G360A perhaps because of its increased surface expression levels (Fig. 3a). The anion currents exhibited by L37P, H542R and I546T EAAT2 were very similar to those of WT EAAT2, both with and without external L-Glu, and thus none of these variants appear to affect EAAT2 anion conductance (Fig. 8).

Fig. 9 and Supplementary Fig. S4 provide correlation plots of the anion currents displayed by WT and variant transporters vs. their cell surface expression levels and transport capacities in this (Fig. 9a and b) and in a previous study[24] (Supplementary Fig. S4a and b). While the anion current densities displayed by most of the transporters correlate with their respective cell surface expression levels, the I276S and A439V variants deviate from this correlation (Fig. 9a). The slightly reduced cell surface expression of I276S compared to WT is accompanied by an increased anion current density compared to WT, indicating gain-of-anion channel function. Considering the WT-like cell surface expression of A439V, the reduced anion currents of this variant must be due to changes in protein function, and the Ala-to-Val substitution in this position thus seems to be equally detrimental to both EAAT2 transport and anion channel functions (Figs. 4a, 5 and 9a). I276S and G360A are two outliers in the correlation plot between the anion current densities and the transport capacities (D-Asp V_{max}) of the transporters (Fig. 9b), suggesting that increased anion channel activity may be caused by the stabilization of anion conducting intermediate conformation of EAAT2 on the expense of conformations driving the substrate translocation through the transporter. Finally, the variants L37P, H542R, and

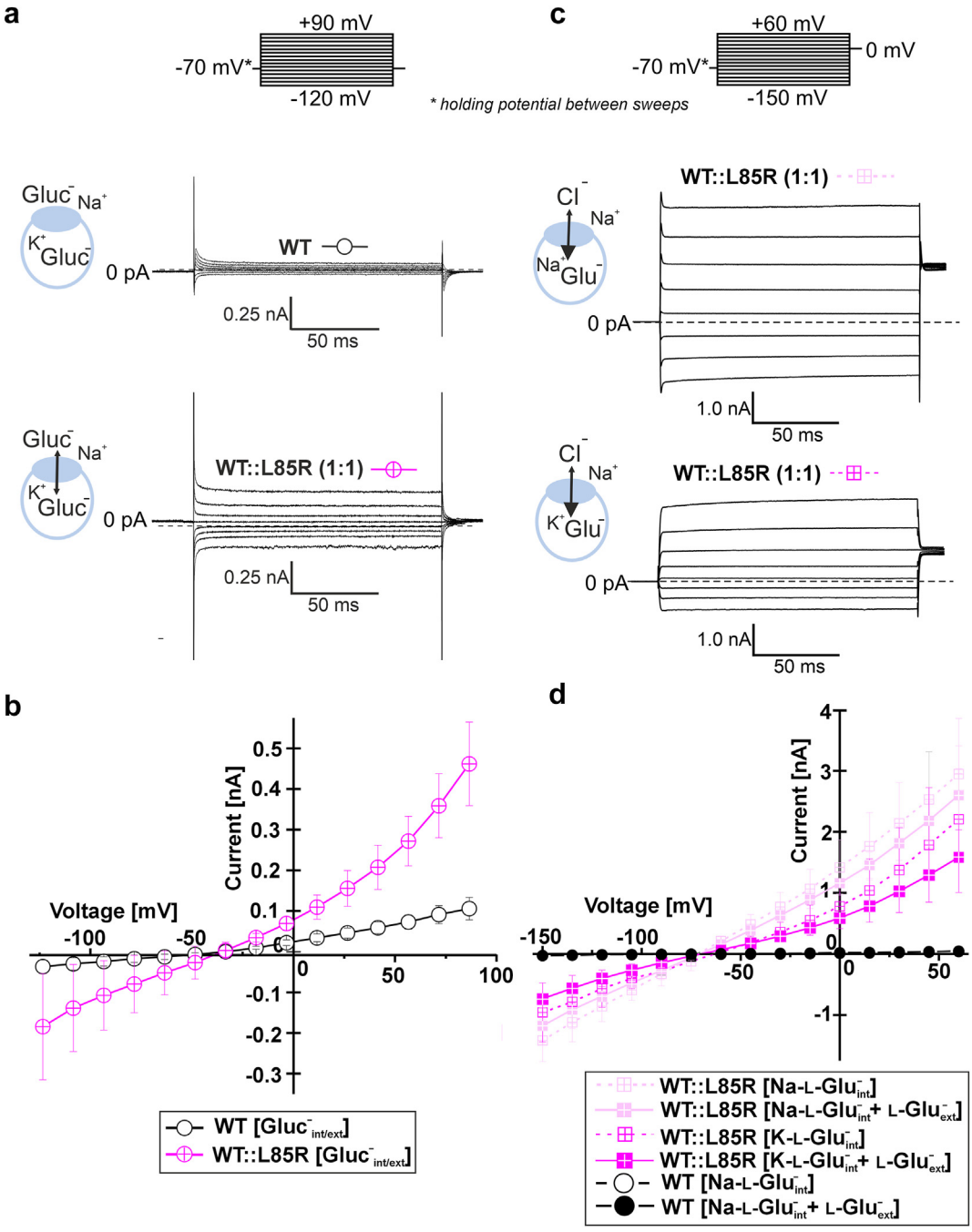

Fig. 6: **L85R variant renders the EAAT2 anion channel permeable for L-Glu.** (**a**) Representative whole-cell recordings of HEK293T cells expressing WT EAAT2 alone (top) and co-expressing WT and L85R EAAT2 (bottom). (**b**) Current-voltage relationships of gluconate currents from WT EAAT2 and WT co-expressed together with L85R under ionic conditions as in **a**. (**c**) Whole-cell recordings of HEK293T cells co-expressing WT and L85R EAAT2 at indicated ion compositions with external Na-gluconate and internal K-gluconate with Na^+-L-Glu_{int} (*top*) or K^+-L-Glu_{int} (*bottom*). (**d**) Current-voltage relationships recorded from WT and L85R under biionic conditions (*insert*) with internal L-Glu and external Cl^- show prominent inward currents for L85R EAAT2, but not for WT EAAT2. The reversal potentials indicate that L85R anion channels are permeable for L-Glu ($P_{L\text{-}Glu/Cl}$ = 0.095 ± 0.013 with Na^+_{int}, n = 5 and 0.103 ± 0.042 with K^+_{int}, n = 6). Supplementing the external solution with 0.5 mM L-Glu did not modify the observed reversal potentials ($P > 0.55^{Na+int/K+int}$). Errors represent 95% confidence intervals of current amplitudes or relative permeabilities $L\text{-}Glu^-/Cl^-$.

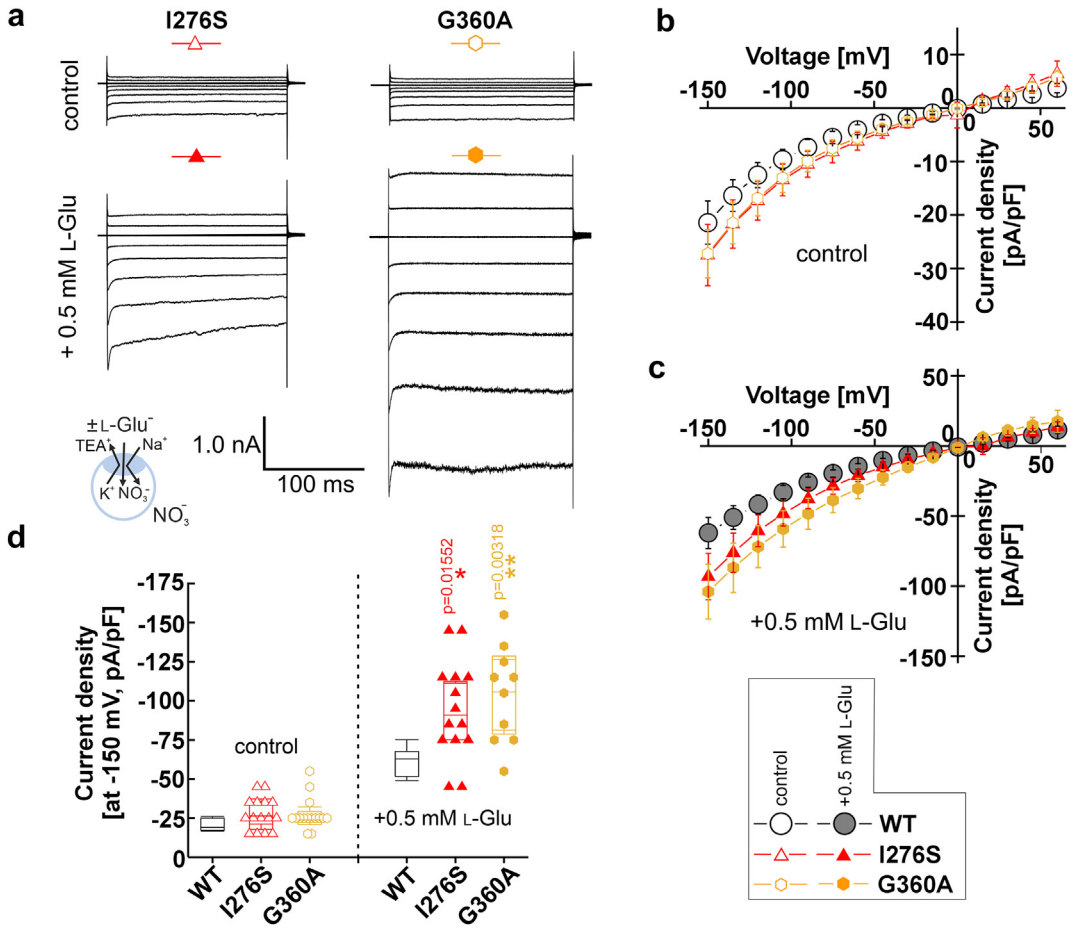

***Fig. 7*: I276S and G360A variants increase EAAT2 anion currents.** (**a**) Representative whole-cell patch clamp recordings from HEK293T cells expressing I276S or G360A EAAT2 in the absence (control, *top*) or in the presence of L-Glu (*bottom*) (**b**) Mean current-voltage relationships from whole cell recordings as shown in Fig. 6a in the absence (**b**) or presence (**c**) of 0.5 mM L-Glu (I276S: wo L-Glu: −27.5 ± 5.7 pA·pF^{-1}, with L-Glu: 93.2 ± 16.5 pA·pF^{-1}, *n* = 15/14; G360A: wo L-Glu: −27.2 ± 4.5 pA·pF^{-1}, with L-Glu: −103.9 ± 19.5 pA·pF^{-1}, *n* = 15/10). (**d**) Statistical analysis of whole cell current densities at −150 mV for WT and variants using *one-way* ANOVAs for each condition and Holm-Sidak *post hoc* testing. Box plots show upper and lower quartiles with data medians, and all error bars and whiskers span 95% confidence intervals of current amplitudes.

I546T causing missense mutations in the EAAT2 N- and C-termini do not differ from expected values for anion current densities, with respect to either cell surface expression (Fig. 9a) or transport function (Fig. 9b).

Phenotypic characterization and genotype-phenotype analysis

The six of the nine novel *SLC1A2* variants found to impact EAAT2 expression and/or function significantly (L37P, H542R and I546T were classified as neutral) and the four previously functionally characterized *SLC1A2* variants[24,31] were classified into three distinct categories based on their molecular phenotypes. The neurological symptoms displayed by the individuals harbouring variants from these three categories are outlined below (Table 2, Supplementary Table S1).

Individuals with "mild gain-of-anion-channel function" variants

Four males harbouring heterozygous I276S or G360A variants were all ambulant without signs of vision impairment, movement disorders, microcephaly, or structural anomalies on MRI. A monozygotic twin pair with the I276S variant both had severe intellectual disability (ID) and epilepsy characterized by onset of focal or bilateral tonic-clonic seizures at the ages of 1 and 10 years, with their EEGs showed multifocal interictal epileptiform discharge as well as background slowing. Both were nonverbal and had autistic features, aggressive behaviour, and no self-care skills, and both presented with feeding difficulties. A father and son harbouring G360A both presented with autistic features but neither suffered from epilepsy.

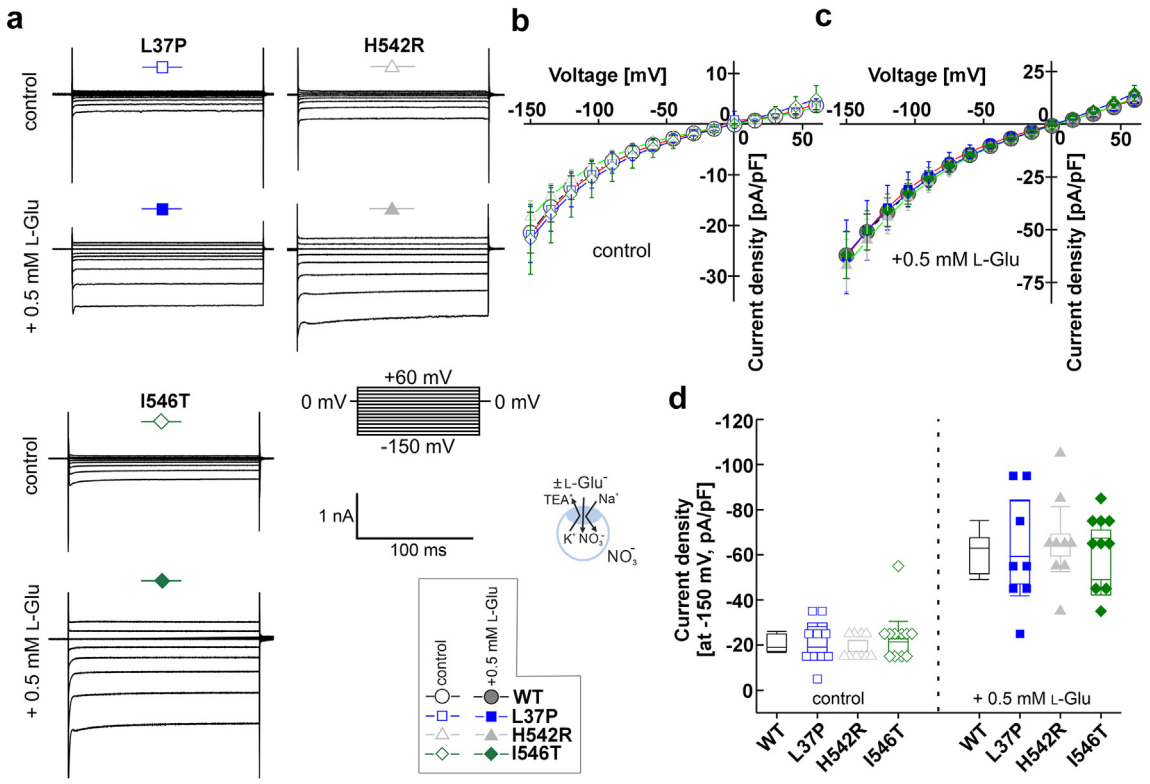

Fig. 8: **L37P, H542R and I546T variants do not alter EAAT2 anion channel function.** (**a**) Representative whole-cell patch clamp recordings from HEK293T cells expressing L37P, H542R or I546T EAAT2 in the absence (control, *top*) or in the presence of 0.5 mM L-Glu (*bottom*). (**b, c**) Mean current-voltage relationships from whole cell recordings as shown in Fig. 7a in the absence (**b**) or presence (**c**) of 0.5 mM L-Glu (L37P: wo L-Glu: −21.8 ± 5.5, with L-Glu: −62.9 ± 17.4 pA·pF^{-1}, *n* = 10/8; H542R: wo L-Glu: −18.3 ± 3.2, with L-Glu: −66.9 ± 12.2 pA·pF^{-1}, *n* = 10/9; I546T: wo L-Glu: −22.7 ± 6.9, with L-Glu: −61.8 ± 11.2 pA·pF^{-1}, *n* = 11/10). **(d)** Statistical analysis of whole cell current densities at −150 mV for WT and variants using *one-way* ANOVAs for each condition and Holm-Sidak *post hoc* testing. Box plots show upper and lower quartiles with data medians and all error bars and whiskers span 95% confidence intervals of current amplitudes.

The father displayed no neurological symptoms and had normal intelligence, whereas the son had moderate ID, was nonverbal and had delayed fine motor development.

Individuals with "loss-of-function" variants

Four individuals (one female, three males) harbouring two heterozygous (A432D, F249Sfs*17) and two homozygous (A439V, c.1421+1G>C) variants all suffered from neurodevelopmental impairment and epilepsy with seizure onset between 2 and 4 years of age, the most common seizure types including focal, atonic and bilateral to tonic-clonic seizures. The two heterozygous variant carriers both had severe ID but were able to walk with support and to say a few words. Both had a normal vision, and their MRIs were reported as normal. The two individuals with the homozygous variants either displayed normal intelligence or mild ID, and both were able to walk independently and to talk in full sentences. However, both had severe vision loss, and one had bilateral hypoplasia of the optic nerves. Three of the four individuals had autistic features, and additional features included attention deficit hyperactivity disorder (1/4), tremor (1/4), kyphoscoliosis (1/4), microcephaly (1/4), and feeding difficulties (1/4).

Individuals with "mixed loss-of-transport/gain-of-anion-channel function" variants

Seven individuals (four females, three males) harbouring heterozygous G82R, L85R, L85P or P289R variants all had severe-to-profound ID, were hypotonic, nonverbal and non-ambulant, and suffered from early-infantile DEE or infantile epileptic spasms syndrome with seizure onset between the second day and 2 months of life. Most common seizure types included focal, tonic, myoclonic, epileptic spasms, and bilateral to tonic-clonic seizures, and EEGs showed a variety of abnormalities including focal/multifocal interictal epileptiform discharge or hypsarrhythmia, often with background slowing. MRIs showed delayed or incomplete myelination (6/7) and microcephaly (4/7), with

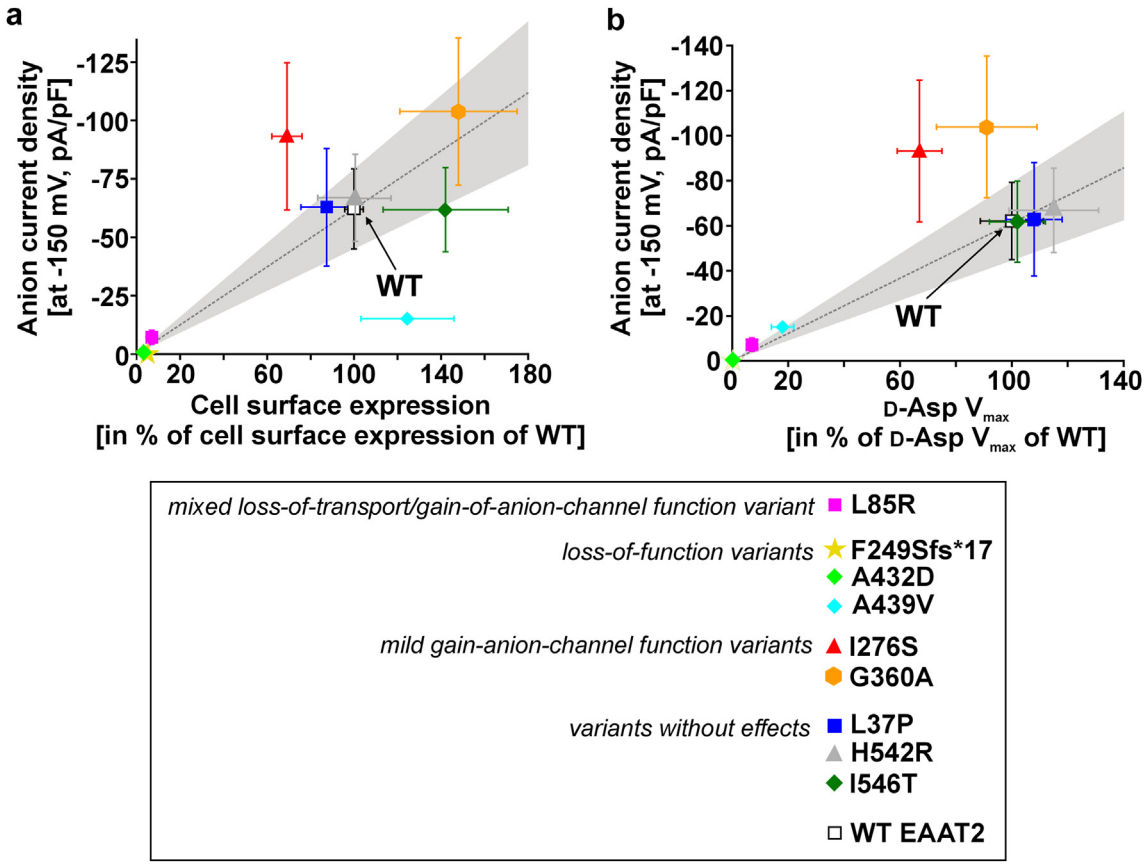

***Fig. 9:* Correlation analyses of WT and variant EAAT2 functional properties.** (**a**) Plot of mean anion current densities at −150 mV (from Figs. 5d, 7d and 8d) vs. normalized cell surface expression levels of the WT and variant transporters (from Fig. 3a) (**b**) Plot of mean anion current densities at −150 mV (from Figs. 5d, 7d and 8d) vs. the D-Asp V_{max} values for the WT and variant transporters (from Table 1). The dashed lines indicate the extrapolated mean values of X-axis values starting from zero and the grey shaded area indicates the extrapolated S.D. for the X-axis values for every level.

neurological/clinical examinations revealing spasticity (5/7), kyphoscoliosis (3/7), nystagmus (2/7), hyperkinetic movement disorder (1/7), and blindness or cortical vision impairment (4/5). Several (3/5) had severe feeding difficulties, with two of them presenting with profound growth failure.

Discussion

In this study we provide a comprehensive analysis of the molecular and clinical phenotypes induced by all *SLC1A2* variants reported to date and propose genotype-phenotype correlations for them.

SLC1A2 variants induce distinct changes in EAAT2 function

While three of the nine novel *SLC1A2* variants leave EAAT2 expression and function unaffected, we observed a diverse spectrum of changes for the remaining six novel variants. The molecular phenotypes of these six variants and four previously published variants[24,27–31] can be classified into three overall categories:

Loss-of-function

All four variants in this category cause robust reductions in both EAAT2 transport and anion channel function. The protein changes arising from the F249Sfs*17 and c.1421+1G>C variants are detrimental for both EAAT2 overall and surface expression levels, and the negligible surface expression of the A432D variant is not enhanced substantially even when the variant incorporated into WT/A432D heterotrimers (Figs. 2 and 3a,b).[31] Whereas neither F249Sfs*17 nor A432D impacted cell surface expression levels or transport capacity of WT EAAT2 in WT::variant-expressing cells significantly in the ELISA and [^{3}H]-D-Asp uptake assay (Figs. 3c and 4d, Table 1), EAAT2 L-Glu transport currents were significantly reduced in WT/F249Sfs*17- and WT/A432D-expressing cells to those of WT EAAT2 alone (Supplementary Fig. S1b–d). We ascribe this apparent difference to

	Loss-of-Function (n = 4)	Mild Gain-of-Anion-Channel-Function (n = 4)	Mixed Loss-of-Transport/Gain-of-Anion-Channel Function (n = 7)
SLC1A2 variants (number of patients)	Heterozygous p.(Phe249Serfs*17) (1), p.(Ala432Asp) (1) Homozygous p.(Ala439Val) (1), c.1421+1G>C (1)	Heterozygous p.(Ile276Ser) (2), p.(Gly360Ala) (2)	Heterozygous p.(Gly82Arg) (3), p.(Leu85Arg) (1) p.(Leu85Pro) (2), p.(Pro289Arg) (1)
Gender	1 female/3 male	4 male	4 female/3 male
Age, average (y)	9 (range 5 y–12 y)	18 (range 5 y–44 y)	9.4 (range 20 m–17 y)
Epilepsy	4/4 (100%)	2/4 (50%)	7/7 (100%)
Average age of seizure onset.	2.7 y (range 24 m–48 m)	5.5 y (range 1 y–10 y)	21 d (range 1 d–2 m)
Diagnosis/syndrome	Focal epilepsy 1/4 (25%) NDD + epilepsy 3/4 (75%)	ASD 1/4 (25%) NDD + ASD 1/4 (25%) NDD + epilepsy 2/4 (50%)	EIDEE 5/7 IESS 2/7
DD/ID	Normal: 1/4 (25%) Mild: 1/4 (25%) Severe: 2/4 (50%)	Normal: 1/4 (25%) Moderate: 1/4 (25%) Severe: 2/4 (50%)	Severe DD: 1/7 (14%) Severe-profound DD: 6/7 (86%)
Language impairment	Normal (full sentences): 2/4 (50%) Severe (few words): 2/4 (50%)	Normal (full sentences): 1/4 (25%) Severe (few words): 1/4 (25%) Profound (nonverbal): 2/4 (50%)	Profound (nonverbal): 5/7 (71%) Unknown: 2/7 (29%)
Gait	Walking independently: 2/4 (50%) Unsteady gait: 2/4 (50%)	Walking independently: 4/4 (100%)	Non-ambulant: 5/7 (71%) Unknown: 2/7 (29%)
Neurological findings	Tremor: 1/4 (25%)	Spasticity: 1/4 (25%)	Hypotonia: 7/7 (100%) Spasticity: 5/7 (71%) Nystagmus: 2/7 (29%)
Dyskinesia/hyperkinesia	3/4 (75%)	0/4 (0%)	1/7 (14%)
Neuro-psychiatric/behavioural features	3/4 (75%)	4/4 (100%)	0/7 (0%)
Microcephaly	1/4 (25%) Unknown: 1/4 (25%)	0/4 (0%)	3/7 (43%) Unknown: 1/7 (14%)
MRI findings	Delayed myelination: 1/4 (25%) Hypoplasia of the optic nerves: 1/4 (25%)	Normal: 2/4 (50%) Unknown: 2/4 (50%)	Normal: 1/7 (14%) Delayed myelination: 6/7 (86%) Cerebral atrophy: 3/7 (43%)
Vision impairment	2/4 (50%)	0/4 (0%)	4/7 (57%) Unknown: 2/7 (29%)

"n" indicates number of patients. ASD, autism spectrum disorder; d, days; DD, developmental delay; EIDEE, early infantile developmental and epileptic encephalopathy; IESS, infantile epileptic spasms syndrome; ID, intellectual disability; m, months; MRI, magnetic resonance imaging; NDD, neurodevelopmental disorder; y, years.

Table 2: **Summary of phenotypic characteristics of 15 patients with pathogenic loss-of-function, mild gain-of-anion-channel-function or mixed loss-of-transport/gain-of-anion-channel function *SLC1A2* variants.**

differences in the methods applied in these assays, and the overall conclusion extracted from all three assays is that overall EAAT2 expression levels and transport capacity in heterozygous carriers of these two variants are profoundly reduced compared to the homozygous WT/WT individual. In contrast to these expression-based reductions in transport capacity in the heterozygous F249Sfs*17 and A432D carriers, the compromised transport capacity and anion conductance of the homozygous A439V variant is not based in changed expression levels but instead arise from a direct effect of this variation on EAAT2 function, and it seems plausible that introduction of bulk (Ala-to-Val) in this position could impact the composition of the closely located substrate binding site and/or the subsequent translocation process.[7]

Mild gain-of-anion-channel function

The I276S and G360A variants mediate modestly increased EAAT2 anion currents, and while I276S also causes a small reduction in transport capacity, G360A does not exhibit significantly altered transport function (Table 1, Figs. 2, 3, 4a,b, 7, and 9). Our studies of the transport properties in WT::I276S- and WT::G360A-expressing cells strongly indicate overall EAAT2 expression levels and transport capacities most likely are relatively unaffected in heterozygous carriers of these variants, and that the gain-of-anion-channel activity thus is the main contributor to the clinical phenotypes in these individuals.

Mixed loss-of-transport/gain-of-anion-channel function

The pronounced changes in EAAT2 anion channel function induced by the G82R, L85R/P and P289R variants make sense in view of the location of these residues in the transporter. Gly82 and Leu85 are TM2 pore-forming residues in the anion conduction pathway, and positively charged sidechains (G82R, L85R) or less aliphatic bulk (L85P) in these positions appear to facilitate anion conductance.[12] As for the membrane-facing

Pro289 in TM5,[7] a P208R mutation in archaeal EAAT homolog Glt_{Tk} (corresponding to P289R in EAAT2) has been proposed to stabilize an anion-conducting transporter conformation via the arginine's interactions with phospholipids.[57]

These four variants affect both EAAT2 transport and anion channel functions, each with distinct cellular functions. At present, we can only speculate which transporter defect is more important in causing epilepsy. As is the major L-Glu uptake carrier in the human brain, substantially reduced EAAT2 transport might increase extracellular L-Glu levels and cause neuronal hyperexcitability. However, the disease symptoms of individuals harbouring variants causing *"mixed loss-of-transport/gain-of-anion-channel function"* are more severe than symptoms caused by the *"loss-of-function"* variants, suggesting that anion channel gain of function is an important pathogenic factor.

At present, cellular functions of glial EAAT anion channels under normal as well as under pathological conditions are insufficiently understood. EAAT1 and EAAT2 anion channels contribute to the regulation of intracellular [Cl^-] in certain glial cells,[58,59] and gain-of-anion-channel function EAAT2 variants might thus reduce intracellular [Cl^-] in these cells. A possible consequence of changes in intracellular Cl^- homoeostasis was recently illustrated in an animal model for episodic ataxia 6. This disease is caused by variants in *SLC1A3*,[60] and many of the disease-associated mutations increase EAAT1 anion conduction.[18,20,21] The episodic ataxia 6-causing P290R EAAT1 variant[60] causes loss-of-transport/gain-of-anion-channel function of EAAT1, quite similar to P289R EAAT2. In $Slc1a3^{P290R/+}$mice, the gain-of-function of EAAT1 anion channels results in glial apoptosis during development—most likely by triggering cell shrinkage via excessive Cl^- efflux after the onset of glutamatergic synaptic transmission–and cerebellar degeneration that causes ataxia.[19] *SLC1A2* variants causing gain-of-function of EAAT2 anion channel function might thus modify glial morphologies and interactions, resulting in changes of synaptic connections in the developing brain.

Some differences are noted when it comes to the impact of the four "*loss-of-transport/gain-of-anion-channel function*" variants on EAAT2 expression. Co-expression of WT and L85R EAAT2 in cells does not increase variant surface expression to levels close to that of the WT transporter (Fig. 3a and b), and thus the co-presence of the WT protein in the cell does not substantially change the low overall expression levels or the intracellular retention of the variant protein. The G82R and L85P variants yield more modest reductions in EAAT2 surface expression levels.[24] The L-Glu permeability exhibited by heterotrimeric WT/L85R transporters (Fig. 6) suggest that heterozygous L85R carriers, analogously to heterozygous G82R or L85P carriers,[24] express a L-Glu efflux pathway. While P289R does not cause EAAT2-mediated L-Glu efflux, it increases EAAT2 anion conductance while reducing its cell surface expression and transport activity.[18,24] The more pronounced reductions in EAAT2 surface expression caused by L85R and P289R than by G82R and L85P could be important for their respective clinical implications. Albeit admittedly speculative, the gain-of-anion-channel component could contribute more prominently to the clinical outcomes in heterozygous carriers of the higher expressed G82R and L85P variants than in heterozygous carriers of the lower expressed L85R and P289R, for whom the loss-of-transport component conversely could be of relative higher importance.

Variants with insignificant effects on EAAT2 function

The fact that L37P, H542R and I546T do not change EAAT2 expression or function is not particular surprising given their locations in the amino- or carboxyl-termini domains.[5] However, these domains in EAATs have been proposed to interact with various intracellular proteins,[61–64] and we cannot rule out that these variants in some way could affect these interactions and through this impact EAAT2 expression and/or function *in vivo*. Alternatively, the clinical phenotypes of individuals harbouring these *SLC1A2* variants could be rooted in different factors.

Genotype-phenotype analysis of *SLC1A2* variants

While the clinical phenotypes in our cohort vary, there is a clear correlation between the distinct changes in EAAT2 function induced by the variants and the specific symptoms and disease severity observed in the affected individuals (Table 2, Supplementary Table S1).

Individuals with heterozygous I276S or G360A variants producing the "*mild gain-of-anion-channel function*" molecular phenotype exhibit no or very mild impairment of motor skills, but a range of cognitive (I276S and G360A) and epileptic (I276S) traits. The difference between these two variants when it comes to induction of epilepsy symptoms is notable. Moreover, the presence of two heterozygous G360A carriers in gnomAD v4.0 also means that this variant must be classified as a VUS, and thus induction of a clinical phenotype by this variant may depend on individual differences and/or compensatory mechanisms. While the moderately increased EAAT2 anion conductance induced by I276S and G360A is unlikely to trigger astrocytic/neuronal death or notable brain abnormalities.[18,24] increased constitutive Cl^- efflux under physiological conditions may change internal anion compositions. Although these two variants induce the mildest clinical phenotypes in our cohort, it is remarkable that modestly augmented anion conductance in one of the allele products in these individuals produce these symptoms.

The four individuals harbouring the heterozygous F249Sfs*17 or A432D or homozygous A439V or c.1421+1G>C variants inducing the "*loss-of-function*"

molecular phenotype display clinical phenotypes of intermediate severity compared to the two other categories. Interestingly, there is some heterogeneity in the specific symptoms observed in this category, as the two individuals harbouring the homozygous variants display normal intelligence or mild ID while both suffering from vision loss, whereas the two individuals with the heterozygous variants are considerably more cognitively impaired but do not exhibit vision loss. In all four individuals, both EAAT2-mediated L-Glu uptake and anion conductance are likely to be profoundly reduced, be it due to lower overall EAAT2 expression (c.1421+1G>C, F249Sfs*17, A432D) or to reduced transporter function (A439V), and the increased synaptic L-Glu concentrations arising from reduced EAAT2 transport throughout the CNS would be expected to impact a range of cognitive, sensory, and motor functions. Paradoxically, the reduced anion channel function induced by these variants could in fact serve to alleviate the impact of these elevated extracellular L-Glu levels on EAAT2 anion conductance, judging from the more severe clinical outcomes caused by the "*mixed loss-of-transport/gain-of-anion-channel function*" variants. A439V is the least functionally compromised variant in this category, but homozygous A439V carriers would certainly be expected to have markedly reduced EAAT2 function and thus elevated L-Glu levels, whereas the presence of six heterozygous A439V carriers in gnomAD v4.0 strongly suggests that this variant only is pathogenic in its homozygous state. In contrast, the presence of a WT *SLC1A2* allele in the heterozygous F249Sfs*17 and A432D carriers is clearly not able to compensate for the reduced expression of the variant allele product. Finally, the relatively mild symptoms exhibited by the individual harbouring the homozygous c.1421+1G>C variant that eliminates EAAT2 expression completely is a surprising finding, considering the key role of the transporter for central L-Glu uptake. This importance is also reflected in the fact that homozygous *Slc1a2*–/– mice combine severe epilepsy with neurodegeneration from reduced glial L-Glu uptake.[65] The clinical phenotype of the homozygous c.1421+1G>C carrier thus indicates that compensatory mechanisms may have been engaged in this individual, such as altered transcriptional expression of genes for other glutamatergic mediators (be it other EAATs, glutamatergic receptors, or enzymes involved in L-Glu biosynthesis or metabolism), changes in the plasma membrane expression of various ion channels, or the resetting of other parameters in the glutamatergic synapse.

Individuals harbouring the heterozygous G82R, L85P, L85R or P289R variants inducing the "*mixed loss-of-transport/gain-of-anion-channel function*" molecular phenotype presented with by far the most severe clinical outcomes (early infantile DEE, profound intellectual disability, non-ambulant and nonverbal) in our cohort. The absence of microcephaly in all three G82R carriers and the pronounced microcephaly observed in three out of four L85R, L85P or P289R carriers was notable, and it may indicate that the L-Glu efflux pathway generated by G82R and L85P/R is not the main reason for this neurological disorder. Blindness or cortical vision impairment was frequently observed in these individuals. Similar features were also observed in some individuals in the "*loss-of-function*" category, suggesting that this trait might arise from the loss-of-transport component. The reduced EAAT2 transport capacity exhibited by all variants in this category, supplemented by the direct EAAT2-mediated L-Glu efflux from presynaptic terminals and astrocytes caused by G82R, L85R and L85P, is bound to increase extracellular L-Glu levels and lead to augmented glutamatergic neurotransmission and excitotoxicity throughout the brain. Furthermore, the markedly more severe clinical outcomes in these individuals compared to those in individuals harbouring "*loss-of-function*" variants underline that the increased anion channel function in the variants from this category is a key pathogenic factor.

Study limitations

Given the rarity of *SLC1A2* variants and this genetic disorder, it is important to recognize the inherent challenges in assembling a large and fully representative cohort. As with many studies of rare disorders, the sample size in this study is limited, even though the inclusion of 18 cases constitutes a substantial proportion of known cases. Although our work provides significant insights, caution is thus warranted when generalizing the results as our cohort may have missed certain phenotypic variants or overrepresented particular traits due to sampling limitations. This is a known and common challenge in rare disease studies. We also acknowledge that patients identified through specialist centres may not fully reflect the broader spectrum of affected individuals, as milder or atypical cases are potentially underrepresented due to diagnostic referral patterns. Ultimately, this study is an important contribution toward identifying key trends and offers valuable insights into the phenotypic variability and genetic mechanisms, but it is not a definitive characterization of the disorder. Additional studies involving larger, more diverse cohorts is needed to validate these findings and to explore full phenotypic spectrum of this genetic disorder.

Conclusion

Here we report the consequences of the thirteen *SLC1A2* variants reported to date on EAAT2 expression, transport and anion channel properties and classify them into three overall molecular phenotype categories. We observe clear correlations between the variant-induced effects on EAAT2 function and the clinical phenotypes presented by individuals harbouring them.

Thus, our findings illustrate heterogeneous effects of *SLC1A2* variants on EAAT2 function and demonstrate how distinct functional changes at the molecular level translate into different clinical phenotypic traits and disease severities. It should be stressed that cases of *SLC1A2* variant-associated disorders are rare and that out cohort consequently is small. Nevertheless, we propose that the genotype/phenotype correlation analysis presented here may provide the foundation for future predictions of disease progression and severity of neurodevelopmental disorders and developmental and epileptic encephalopathies in individuals harbouring *SLC1A2* variants, and that our findings also could aid individualised treatment of these individuals.

Contributors

PK, AB, ChF, RSM and AAJ conceptualized and designed the study and acquired funding. PK, ChF and AAJ performed the expression and functional studies (generated cDNA constructs and performed confocal microscopy, ELISA, uptake assays and electrophysiological recordings) and collected, analysed, and interpreted data from these. AB, CDF, LL, AB, AS, VL, GL, LP, JL and RSM recruited and phenotyped patients. PK, AB, ChF, RSM and AAJ interpreted and curated data (genotype-phenotype correlation analysis). PK, AB, ChF, RSM and AAJ accessed and verified data. PK, AB, ChF, RSM and AAJ produced figures and tables and wrote the manuscript. All authors revised and approved the final manuscript.

Data sharing statement

All data are available within the main text or in the Supplementary materials. Data from the confocal microscopy and electrophysiology experiments are available on GitHub: https://github.com/peterkovermann/epileptic_encephalopathy_2. Clinical information associated with this study and all other data are available from the corresponding author upon reasonable request. Data will be stored for a minimum of 7 years.

Declaration of interests

RSM has received consulting fees from UCB, Orion, Saniona and Immedica, and speaker fees from EISAI, Angelini Pharma, Jazz Pharmaceuticals, Orion and UCB. The remaining authors declare no competing interests.

Acknowledgements

We thank the patients and families who participated in the collection of clinical data for this project and for enrolling in our research studies. Drs. M. Hediger (Universität Bern, Switzerland) and S.G. Amara (National Institutes of Health, Bethesda, MD) are thanked for their generous gifts of EAAT2 cDNAs. AAJ was supported by the Lundbeck Foundation, and ChF was supported by the German Ministry of Education and Research (BMBF 01GM2210D, E-RARE network, Treat-ION).

Appendix A. Supplementary data

Supplementary data related to this article can be found at https://doi.org/10.1016/j.ebiom.2025.105648.

References

1 Kadriu B, Musazzi L, Johnston JN, et al. Positive AMPA receptor modulation in the treatment of neuropsychiatric disorders: a long and winding road. *Drug Discov Today*. 2021;26(12):2816–2838.
2 Kwan C, Kang W, Kim E, Belliveau S, Frouni I, Huot P. Metabotropic glutamate receptors in Parkinson's disease. *Int Rev Neurobiol*. 2023;168:1–31.
3 Chen S, Xu D, Fan L, Fang Z, Wang X, Li M. Roles of N-Methyl-D-Aspartate receptors (NMDARs) in epilepsy. *Front Mol Neurosci*. 2021;14:797253.
4 Danbolt NC. Glutamate uptake. *Prog Neurobiol*. 2001;65:1–105.
5 Vandenberg RJ, Ryan RM. Mechanisms of glutamate transport. *Physiol Rev*. 2013;93(4):1621–1657.
6 Rose CR, Ziemens D, Untiet V, Fahlke C. Molecular and cellular physiology of sodium-dependent glutamate transporters. *Brain Res Bull*. 2018;136:3–16.
7 Kato T, Kusakizako T, Jin C, et al. Structural insights into inhibitory mechanism of human excitatory amino acid transporter EAAT2. *Nat Commun*. 2022;13(1):4714.
8 Qiu B, Boudker O. Symport and antiport mechanisms of human glutamate transporters. *Nat Commun*. 2023;14(1):2579.
9 Zerangue N, Kavanaugh MP. Flux coupling in a neuronal glutamate transporter. *Nature*. 1996;383(6601):634–637.
10 Alleva C, Machtens JP, Kortzak D, Weyand I, Fahlke C. Molecular basis of coupled transport and anion conduction in excitatory amino acid transporters. *Neurochem Res*. 2022;47(1):9–22.
11 Wadiche JI, Amara SG, Kavanaugh MP. Ion fluxes associated with excitatory amino acid transport. *Neuron*. 1995;15(3):721–728.
12 Machtens JP, Kortzak D, Lansche C, et al. Mechanisms of anion conduction by coupled glutamate transporters. *Cell*. 2015;160(3):542–553.
13 Kovermann P, Engels M, Müller F, Fahlke C. Cellular physiology and pathophysiology of EAAT anion channels. *Front Cell Neurosci*. 2021;15:815279.
14 Chen I, Pant S, Wu Q, et al. Glutamate transporters have a chloride channel with two hydrophobic gates. *Nature*. 2021;591(7849):327–331.
15 Kovermann P, Machtens JP, Ewers D, Fahlke C. A conserved aspartate determines pore properties of anion channels associated with excitatory amino acid transporter 4 (EAAT4). *J Biol Chem*. 2010;285(31):23676–23686.
16 Fiorentino A, Sharp SI, McQuillin A. Association of rare variation in the glutamate receptor gene *SLC1A2* with susceptibility to bipolar disorder and schizophrenia. *Eur J Hum Genet*. 2015;23(9):1200–1206.
17 Zhang B, Guan F, Chen G, et al. Common variants in *SLC1A2* and schizophrenia: association and cognitive function in patients with schizophrenia and healthy individuals. *Schizophr Res*. 2015;169(1–3):128–134.
18 Winter N, Kovermann P, Fahlke C. A point mutation associated with episodic ataxia 6 increases glutamate transporter anion currents. *Brain*. 2012;135(Pt 11):3416–3425.
19 Kovermann P, Untiet V, Kolobkova Y, et al. Increased glutamate transporter-associated anion currents cause glial apoptosis in episodic ataxia 6. *Brain Commun*. 2020;2(1):fcaa022.
20 Chivukula AS, Suslova M, Kortzak D, Kovermann P, Fahlke C. Functional consequences of *SLC1A3* mutations associated with episodic ataxia 6. *Hum Mutat*. 2020;41(11):1892–1905.
21 Wu Q, Akhter A, Pant S, et al. Ataxia-linked *SLC1A3* mutations alter EAAT1 chloride channel activity and glial regulation of CNS function. *J Clin Invest*. 2022;132(7).
22 Petr GT, Sun Y, Frederick NM, et al. Conditional deletion of the glutamate transporter GLT-1 reveals that astrocytic GLT-1 protects against fatal epilepsy while neuronal GLT-1 contributes significantly to glutamate uptake into synaptosomes. *J Neurosci*. 2015;35(13):5187–5201.
23 Rimmele TS, Rosenberg PA. GLT-1: the elusive presynaptic glutamate transporter. *Neurochem Int*. 2016;98:19–28.
24 Kovermann P, Kolobkova Y, Franzen A, Fahlke C. Mutations associated with epileptic encephalopathy modify EAAT2 anion channel function. *Epilepsia*. 2022;63(2):388–401.
25 Alijanpour S, Miryounesi M, Ghafouri-Fard S. The role of excitatory amino acid transporter 2 (EAAT2) in epilepsy and other neurological disorders. *Metab Brain Dis*. 2023;38(1):1–16.
26 Zaitsev AV, Smolensky IV, Jorratt P, Ovsepian SV. Neurobiology, functions, and relevance of excitatory amino acid transporters (EAATs) to treatment of refractory epilepsy. *CNS Drugs*. 2020;34(11):1089–1103.
27 Allen AS, Berkovic SF, Cossette P, et al. *De novo* mutations in epileptic encephalopathies. *Nature*. 2013;501(7466):217–221.
28 Guella I, McKenzie MB, Evans DM, et al. *De Novo* mutations in YWHAG cause early-onset epilepsy. *Am J Hum Genet*. 2017;101(2):300–310.
29 De Novo Mutations in *SLC1A2* and *CACNA1A* are important causes of epileptic encephalopathies. *Am J Hum Genet*. 2016;99(2):287–298.
30 Stergachis AB, Pujol-Giménez J, Gyimesi G, et al. Recurrent *SLC1A2* variants cause epilepsy via a dominant negative mechanism. *Ann Neurol*. 2019;85(6):921–926.

31 Wagner M, Gusic M, Günthner R, et al. Biallelic mutations in *SLC1A2*; an additional mode of inheritance for *SLC1A2*-related epilepsy. *Neuropediatrics*. 2018;49(1):59–62.
32 Rinaldi B, Bayat A, Zachariassen LG, et al. Gain-of-function and loss-of-function variants in GRIA3 lead to distinct neurodevelopmental phenotypes. *Brain*. 2024;147(5):1837–1855.
33 Specchio N, Wirrell EC, Scheffer IE, et al. International league against epilepsy classification and definition of epilepsy syndromes with onset in childhood: position paper by the ILAE task force on nosology and definitions. *Epilepsia*. 2022;63(6):1398–1442.
34 Zuberi SM, Wirrell E, Yozawitz E, et al. ILAE classification and definition of epilepsy syndromes with onset in neonates and infants: position statement by the ILAE Task Force on Nosology and Definitions. *Epilepsia*. 2022;63(6):1349–1397.
35 Richards S, Aziz N, Bale S, et al. Standards and guidelines for the interpretation of sequence variants: a joint consensus recommendation of the American College of medical genetics and genomics and the association for molecular pathology. *Genet Med*. 2015;17(5):405–424.
36 Ioannidis NM, Rothstein JH, Pejaver V, et al. REVEL: an ensemble method for predicting the pathogenicity of rare missense variants. *Am J Hum Genet*. 2016;99(4):877–885.
37 Kircher M, Witten DM, Jain P, O'Roak BJ, Cooper GM, Shendure J. A general framework for estimating the relative pathogenicity of human genetic variants. *Nat Genet*. 2014;46(3):310–315.
38 Collins RL, Brand H, Karczewski KJ, et al. A structural variation reference for medical and population genetics. *Nature*. 2020;581(7809):444–451.
39 Karczewski KJ, Francioli LC, Tiao G, et al. The mutational constraint spectrum quantified from variation in 141,456 humans. *Nature*. 2020;581(7809):434–443.
40 den Dunnen JT, Dalgleish R, Maglott DR, et al. HGVS recommendations for the description of sequence variants: 2016 update. *Hum Mutat*. 2016;37(6):564–569.
41 Leinenweber A, Machtens JP, Begemann B, Fahlke C. Regulation of glial glutamate transporters by C-terminal domains. *J Biol Chem*. 2011;286(3):1927–1937.
42 Horton RM, Hunt HD, Ho SN, Pullen JK, Pease LR. Engineering hybrid genes without the use of restriction enzymes: gene splicing by overlap extension. *Gene*. 1989;77(1):61–68.
43 Schindelin J, Arganda-Carreras I, Frise E, et al. Fiji: an open-source platform for biological-image analysis. *Nat Methods*. 2012;9(7):676–682.
44 Madjroh N, Davies PA, Smalley JL, Kristiansen U, Söderhielm PC, Jensen AA. Delineation of the functional properties exhibited by the Zinc-Activated Channel (ZAC) and its high-frequency Thr(128)Ala variant (rs2257020) in Xenopus oocytes. *Pharmacol Res*. 2021;169:105653.
45 Jensen AA, Bräuner-Osborne H. Pharmacological characterization of human excitatory amino acid transporters EAAT1, EAAT2 and EAAT3 in a fluorescence-based membrane potential assay. *Biochem Pharmacol*. 2004;67:2115–2127.
46 Fu H, Zhang J, Tepper PG, Bunch L, Jensen AA, Poelarends GJ. Chemoenzymatic synthesis and pharmacological characterization of functionalized aspartate analogues as novel excitatory amino acid transporter inhibitors. *J Med Chem*. 2018;61(17):7741–7753.
47 Cheng Y, Prusoff WH. Relationship between the inhibition constant (K1) and the concentration of inhibitor which causes 50 per cent inhibition (I50) of an enzymatic reaction. *Biochem Pharmacol*. 1973;22:3099–3108.
48 Kolen B, Borghans B, Kortzak D, et al. Vesicular glutamate transporters are H(+)-anion exchangers that operate at variable stoichiometry. *Nat Commun*. 2023;14(1):2723.
49 Bernstein FC, Koetzle TF, Williams GJ, et al. The Protein Data Bank. A computer-based archival file for macromolecular structures. *Eur J Biochem*. 1977;80(2):319–324.
50 Zhang Z, Chen H, Geng Z, et al. Structural basis of ligand binding modes of human EAAT2. *Nat Commun*. 2022;13(1):3329.
51 Grewer C, Balani P, Weidenfeller C, Bartusel T, Tao Z, Rauen T. Individual subunits of the glutamate transporter EAAC1 homotrimer function independently of each other. *Biochemistry*. 2005;44(35):11913–11923.
52 Leary GP, Stone EF, Holley DC, Kavanaugh MP. The glutamate and chloride permeation pathways are colocalized in individual neuronal glutamate transporter subunits. *J Neurosci*. 2007;27(11):2938–2942.
53 Koch HP, Brown RL, Larsson HP. The glutamate-activated anion conductance in excitatory amino acid transporters is gated independently by the individual subunits. *J Neurosci*. 2007;27(11):2943–2947.
54 Leighton BH, Seal RP, Watts SD, Skyba MO, Amara SG. Structural rearrangements at the translocation pore of the human glutamate transporter, EAAT1. *J Biol Chem*. 2006;281(40):29788–29796.
55 Wadiche JI, Kavanaugh MP. Macroscopic and microscopic properties of a cloned glutamate transporter/chloride channel. *J Neurosci*. 1998;18(19):7650–7661.
56 Melzer N, Biela A, Fahlke C. Glutamate modifies ion conduction and voltage-dependent gating of excitatory amino acid transporter-associated anion channels. *J Biol Chem*. 2003;278(50):50112–50119.
57 Colucci E, Anshari ZR, Patiño-Ruiz MF, et al. Mutation in glutamate transporter homologue GltTk provides insights into pathologic mechanism of episodic ataxia 6. *Nat Commun*. 2023;14(1):1799.
58 Untiet V, Kovermann P, Gerkau NJ, Gensch T, Rose CR, Fahlke C. Glutamate transporter-associated anion channels adjust intracellular chloride concentrations during glial maturation. *Glia*. 2017;65(2):388–400.
59 Engels M, Kalia M, Rahmati S, et al. Glial chloride homeostasis under transient ischemic stress. *Front Cell Neurosci*. 2021;15:735300.
60 Jen JC, Wan J, Palos TP, Howard BD, Baloh RW. Mutation in the glutamate transporter EAAT1 causes episodic ataxia, hemiplegia, and seizures. *Neurology*. 2005;65(4):529–534.
61 Lin CI, Orlov I, Ruggiero AM, et al. Modulation of the neuronal glutamate transporter EAAC1 by the interacting protein GTRAP3-18. *Nature*. 2001;410(6824):84–88.
62 Bassan M, Liu H, Madsen KL, et al. Interaction between the glutamate transporter GLT1b and the synaptic PDZ domain protein PICK1. *Eur J Neurosci*. 2008;27(1):66–82.
63 D'Amico A, Soragna A, Di Cairano E, et al. The surface density of the glutamate transporter EAAC1 is controlled by interactions with PDZK1 and AP2 adaptor complexes. *Traffic*. 2010;11(11):1455–1470.
64 Sogaard R, Borre L, Braunstein TH, Madsen KL, MacAulay N. Functional modulation of the glutamate transporter variant GLT1b by the PDZ domain protein PICK1. *J Biol Chem*. 2013;288(28):20195–20207.
65 Tanaka K, Watase K, Manabe T, et al. Epilepsy and exacerbation of brain injury in mice lacking the glutamate transporter GLT-1. *Science*. 1997;276(5319):1699–1702.